Hindawi Publishing Corporation
Journal of Geological Research
Volume 2013, Article ID 590835, 22 pages
http://dx.doi.org/10.1155/2013/590835

Research Article

Magmatism in the Asunción-Sapucai-Villarrica Graben (Eastern Paraguay) Revisited: Petrological, Geophysical, Geochemical, and Geodynamic Inferences

Piero Comin-Chiaramonti,[1] Angelo De Min,[1] Aldo Cundari,[2] Vicente A. V. Girardi,[3] Marcia Ernesto,[4] Celso B. Gomes,[3] and Claudio Riccomini[3]

[1] *Mathematics and Geosciences Department, Trieste University, Via Weiss 8, 34127 Trieste, Italy*
[2] *Geotrack International, 37 Melville Road, Brunswick West, Melbourne, VIC 3055, Australia*
[3] *Geosciences Institute, University of São Paulo, Cidade Universitária, Rua do Lago 562, 05508-900 São Paulo, SP, Brazil*
[4] *Astronomical and Geophysical Institute (IAG) of the São Paulo University, Rua do Matão 1226, 05508-090 São Paulo, SP, Brazil*

Correspondence should be addressed to Piero Comin-Chiaramonti; comin@units.it

Received 12 November 2012; Revised 25 March 2013; Accepted 8 April 2013

Academic Editor: David T. A. Symons

The Asunción-Sapucai-Villarrica graben (ASV) in Eastern Paraguay at the westernmost part of the Paraná Basin was the site of intense magmatic activity in Mesozoic and Tertiary times. Geological, petrological, mineralogical, and geochemical results indicate that the following magmatic events are dominant in the area: (1) tholeiitic basalt and basaltic andesites, flows and sills of low- and high-titanium types; (2) K-alkaline magmatism, where two suites are distinguished, that is, basanite to phonolite and alkali basalt to trachyte and their intrusive analogues; (3) ankaratrite to phonolite with strong Na-alkaline affinity, where mantle xenoliths in ultramafic rocks are high- and low-potassium suites, respectively. The structural and geophysical data show extensional characteristics for ASV. On the whole, the geochemical features imply different mantle sources, consistently with Sr-Nd isotopes that are Rb-Nd enriched and depleted for the potassic and sodic rocks, respectively. Nd model ages suggest that some notional distinct "metasomatic events" may have occurred during Paleoproterozoic to Neoproterozoic times as precursor to the alkaline and tholeiitic magmas. It seems, therefore, that the genesis of the ASV magmatism is dominated by a lithospheric mantle, characterized by small-scale heterogeneity.

1. Introduction

Velázquez et al. [1] presented a structural analysis of the central segment of the "Asunción Rift," mainly based on the previous papers related to the Eastern Paraguay magmatism in general, and to the Asunción-Sapucai-Villarrica graben (ASV) in particular, and also based on extensive field data collected earlier on the dyke swarms cropping out in the area. However, some aspects as, for example, the close association in space of potassic and sodic alkaline rock-types with tholeiitic dykes and flows (both of high- and low-Ti types; cf. [2]), have not been discussed in detail by the above authors.

This paper focuses on general aspects of the magmatism from the western margin of the Paraná-Angola-Etendeka system (PAE), where tholeiitic flows and dykes (Early Cretaceous, both of high-Ti and low-Ti types; cf. Figure 1(a) and [3]) are associated in time and space with a wide variety of alkaline rock-types (both potassic and sodic) and carbonatites.

The investigated alkaline and tholeiitic rocks from Eastern Paraguay span in age mainly from Early Cretaceous to Paleogene times. Therefore, they are germane to the magmatic and tectonic evolution of the PAE and of the Atlantic Ocean (cf. Figure 1(b) and [4, 5]).

This review aims at discussing (1) the relationships between tectonics and magmatic activity on the basis of field and geophysical data; (2) a detailed description of the geological characteristics of the Asunción-Sapucai-Villarrica

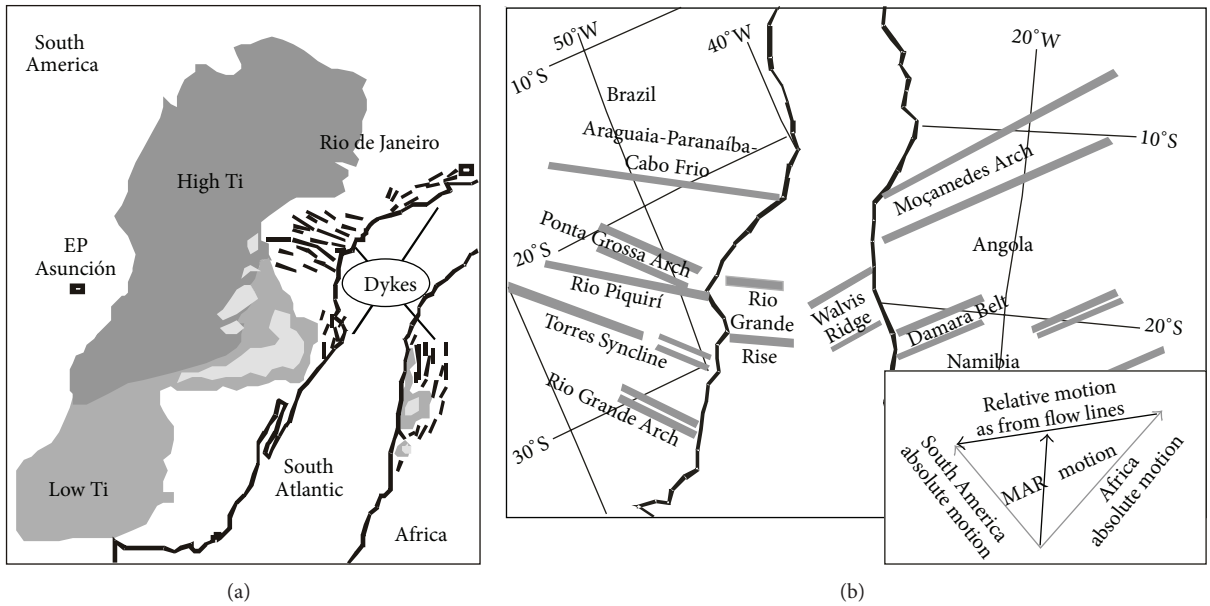

Figure 1: (a) Sketch map of the Paraná-Angola-Etendeka system [3] where the arrows indicate the occurrences of the main dyke swarms. The basaltic lavas are subdivided into broad high- and low-Ti groups and late-stage rhyolites (yellow fields). EP: Eastern Paraguay. (b) Main lineaments in the Paraná-Angola-Etendeka system (PAE), western Gondwana at ca. 110 Ma (modified after [6]), corresponding to the main lineaments of the alkaline and alkaline-carbonatitic complex. Inset: vector diagram showing relationships among absolute plate motions, relative motions, and motion of the Mid-Atlantic Ridge (MAR, after [7]).

(ASV) graben; (3) petrography and petrochemistry of the magmatic rock-types (and the associated mantle xenoliths) from ASV; (4) the most important geochemical and Sr-Nd isotopic features of the magmatism; (5) the petrogenesis and geodynamic implications.

2. Eastern Paraguay: Geological Outlines and Geophysical Aspects

Eastern Paraguay shows a complex block-faulted structure between the southern Precambrian tip of the Amazonian Craton (Apa block) and the northern one of the Rio de la Plata Craton (Caacupú high; Figure 2). This intercratonic area, including the westernmost fringe of the Paraná Basin (PB), represents an undeformed basin along the western Gondwana (Figure 1), where the sedimentation, started in Cambrian times, was topped by Early Cretaceous tholeiitic basalts of the Serra Geral Formation [8, 9] and followed by younger sedimentation (Figure 2).

Moreover, it should be also noted that Eastern Paraguay lies along the former western margin of the Gondwana, bounded by an anticlinal structure established since Early Paleozoic, the Asunción Arch, which separates the Paraná Basin (East) from the Gran Chaco Basin (West) [10]. PB shows a high-velocity upper mantle "lid" with a maximum S-wave velocity of 4.7 km/s (Moho 37 km depth), with an unresolved low-velocity zone to a depth of at least 200 km [11]. Between the two blocks, that is, Apa and Caacupú of Figure 2, Eastern Paraguay was subjected to NE-SW-trending crustal extension during Late Jurassic-Early Cretaceous, probably related to the western Gondwana breakup (Figure 1; [10, 12] and therein references). NW-SE trending faults, paralleling the dominant orientation of Mesozoic alkaline and tholeiitic dykes, reflect this type of structure [13, 14].

From the aeromagnetic survey [15, 16], the linear magnetic anomalies trend mainly N40-45W (Figure 3). These anomalies have been interpreted as resulting from Early Cretaceous tholeiitic dyke swarms [16], but field evidence does not support this hypothesis. Most magnetic anomalies correspond to older Precambrian tectonic lineament [17]. The Landsat lineaments, trending mainly NE and EW, may therefore reflect tectonic lineaments from the basement [18].

The Bouguer gravity map (Figure 3) consists of prevailing NW-trending gravity "highs" and "lows" that represent shallow to exposed basement and sedimentary basins, respectively [19]. The boundaries between gravity highs and lows are generally marked by step gradients that may reflect abrupt basement offsets along faults, or basement dip changes by crustal warping. Notably, the gravity lows and highs parallel the dominant NW attitude of the magnetic lineaments, with post-Palaeozoic magmatism (both tholeiitic and alkaline) associated with gravity lows. Therefore, the ASV represents the most important geological structure of the region (see later).

Notably, the present seismic activity (earthquakes with hypocenters <70 km) indicates that the NW-trending fault systems continue up to present day, that is, the Pilcomayo lineament (inset of Figure 3), also aligned with the Piquirí lineament and the Torres syncline (Figure 1(b)).

In conclusion, the resulting structural pattern controlled the development of grabens or semigrabens as a response to NE-SW-directed extension and continued evolving into Cenozoic times [12, 24]. According to Tommasi and

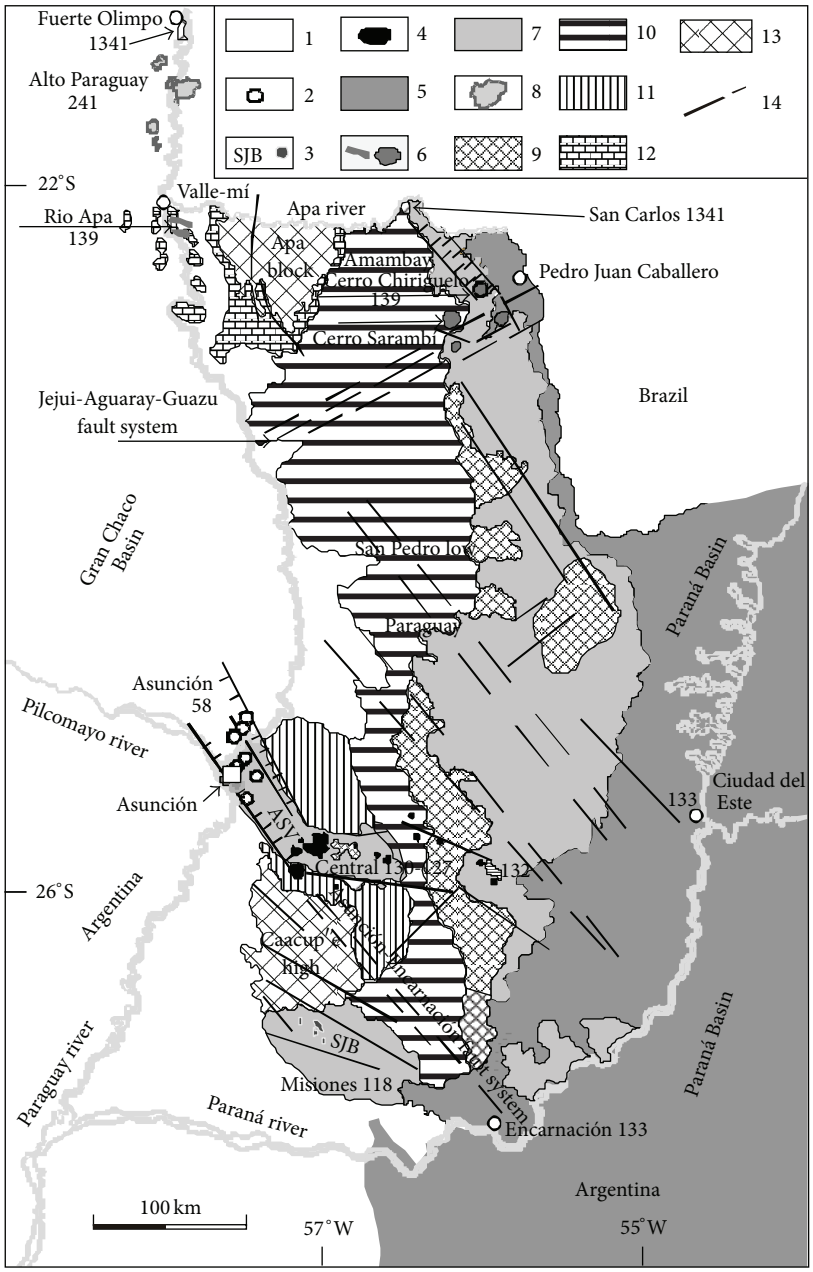

Figure 2: Geological sketch map of Eastern Paraguay (modified after [10, 13, 20–24]). ASV: Asunción-Sapucai-Villarrica graben. (1): Neogene and Paleogene sedimentary cover (e.g., Gran Chaco); (2): Paleogene sodic alkaline rocks, Asunción Province; (3): Late-Early Cretaceous sodic alkaline rocks (Misiones Province, San Juan Bautista, SJB); (4): Early Cretaceous potassic alkaline rocks (posttholeiites; ASU: Asunción-Sapucai-Villarica graben, Central Province); (5): Early Cretaceous tholeiites of the Paraná Basin (Serra Geral Formation in Brazil and Alto Paraná Formation in Paraguay; cf. [4]); (6): Early Cretaceous potassic alkaline rocks (pretholeiites, Apa and Amambay Provinces); (7): Jurassic-Cretaceous sedimentary rocks (Misiones Formation); (8): Permo-Triassic alkaline rocks (Alto Paraguay Province); (9): Permian sedimentary rocks (Independencia Group); (10): Permo-Carboniferous sedimentary rocks (Coronel Oviedo Group); (11): Ordovician-Silurian sedimentary rocks (Caacupé and Itacurubí Groups); (12): Cambro-Ordovician platform carbonates (Itacupumí Group); (13): Archean to Early Paleozoic crystalline basement: high- to low-grade metasedimentary rocks, metarhyolites, and granitic intrusions; (14): major tectonic lineaments and faults. The radiometric values, for example, 133 Ma, are referred to $^{40}Ar/^{39}Ar$ plateau ages for the main magmatic types [25–27] and to Rb/Sr ages for the Precambrian rhyolitic rocks of Fuerte Olimpo and Fuerte San Carlos [28].

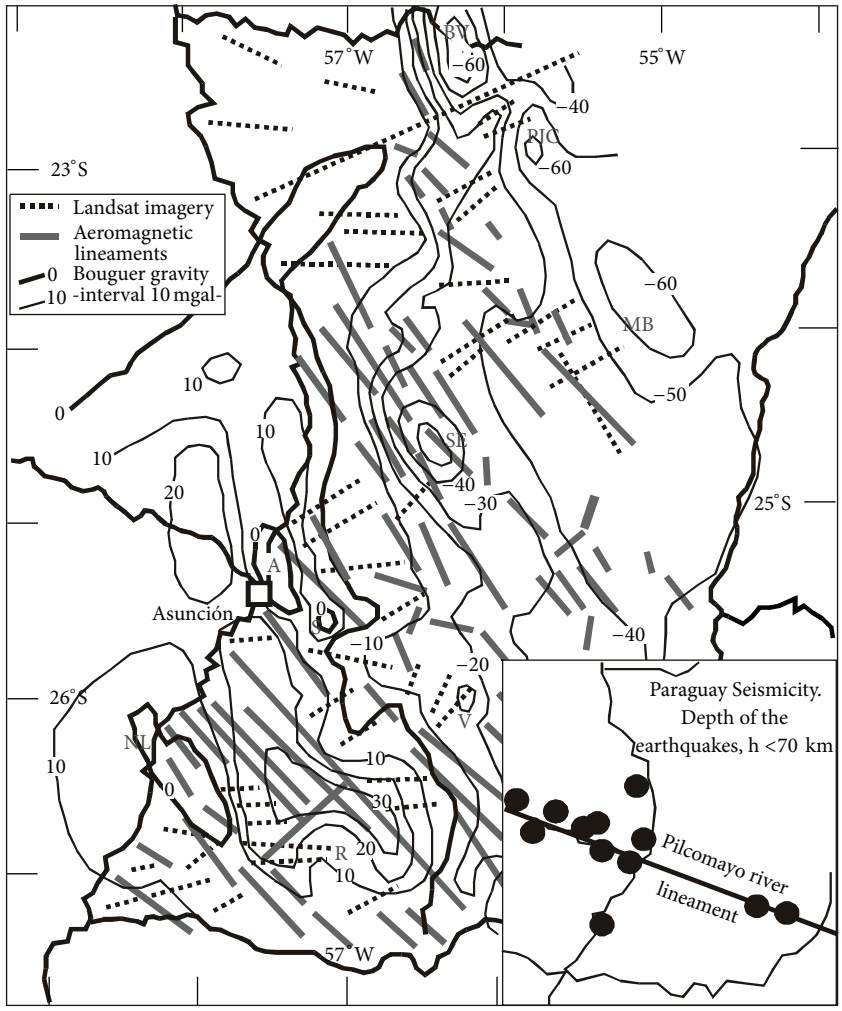

Figure 3: Geological sketch map showing aeromagnetic and Landsat lineaments in Eastern Paraguay and Bouguer gravity data [16–18]. Gravity lows: BV, Bella Vista; PJC, Pedro Juan Caballero; MB, Mbacarayú; SE, San Estanislao (formerly San Pedro); A, Asunción, S, Sapucai, V, Villarrica (ASV graben); R, Santa Rosa. Inset: distribution of earthquakes with depth <70 km [29].

Vauchez [30], rift orientations seem to have been controlled by the preexisting lithospheric mantle fabric, as indicated by deep geophysical data.

The thermal history, using apatite fission track analyses (AFTA), reveals that at least two main episodes have been identified in sedimentary and igneous/metamorphic samples ranging in age from Late Ordovician to Early Cretaceous [31, 32]. AFTA data from ASV show evidence for rapid cooling beginning sometime between 90 and 80 Ma, similar to the results found along Brazilian and Uruguayan coasts. A Tertiary heating/cooling episode is also suggested by AFTA data (60–10 Ma), supporting early work in the area. The time of the first event is significantly younger than any rifting activity related to the Paraná flood basalts and to the opening of the South Atlantic. Late Cretaceous cooling may have involved several kilometers of differential uplift and erosion and would have played an important role in the control of the geomorphology and drainage patterns of the region, especially in the ASV system [31, 32].

Beginning from Mesozoic times (Figure 2), almost five main alkaline magmatic events have occurred in Eastern Paraguay, other than the Early Cretaceous tholeiitic magmatism (133-134 Ma; [4]). Three of these include rocks of sodic affinity, corresponding geographically to the provinces of Alto Paraguay (241.5 ± 1.3 Ma), Misiones (118.3 ± 1.6 Ma), and Asunción (58.7 ± 2.4 Ma), whereas two involve rocks of potassic affinity associated with the Apa and Amambay provinces, both of similar age (138.9 ± 0.7), and with the Central Province (ASV, 126.4 ± 0.4 Ma).

3. Asunción-Sapucai-Villarrica Graben (ASV)

The ASV graben (Figure 4) is the dominant rifting structure in Eastern Paraguay, linked to NE-SW extensional vectors [13], and it is characterized by a gravity anomaly trending N30-45W near Asunción townships (Figure 3). The graben, nearly symmetrical and defined by major faults along each margin [1, 12, 18, 37], may be subdivided into three main

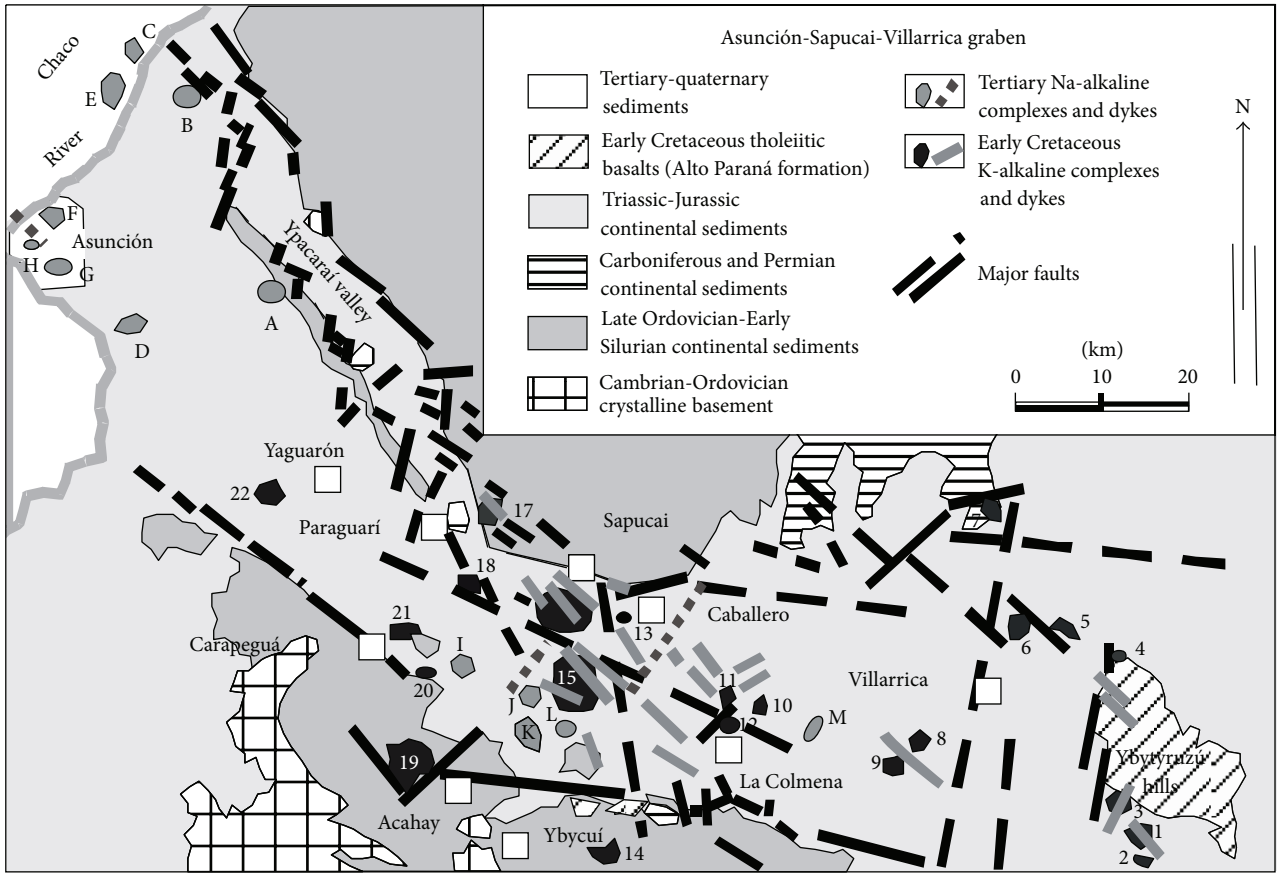

Figure 4: Geological sketch map of the Asunción-Sapucai-Villarrica graben showing the main occurrences of magmatic rock-types, modified after [33]. In parentheses preferred K/Ar and plateau Ar/Ar ages (in bold) in Ma according to [4, 33]. *K-alkaline complexes*: 1, Cerro Km 23 (132, **128**); 2, Cerro San Benito (**127**); 3, Cerro E. Santa Elena (**126**); 4, Northwestern Ybytyruzú (125–129); 5, Cerro Capiitindy (n.a.); 6, Mbocayaty (126–130, **126**); 7, Aguapety Portón (128–133, **126**); 8, Cerro Itapé (n.a.); 9, Cerrito Itapé (n.a.); 10, Cerro Cañada (**127**); 11, Cerro Chobí (n.a.); 12, Potrero Garay (n.a.); 13, Catalán (n.a.); 14, Cerro San José (**127**); 15, Potrero Ybaté (126–128, **128**); 16, Sapucai (119–131, **126**); 17, Cerro Santo Tomás (126–130, **127**); 18, Cerro Porteño (n.a.); 19, Cerro Acahay (118, **127**); 20, Cerro Pinto (n.a.); 21, Cerro Ybypyté (124); 22, Cerro Arrúa-í (126–132, **129**). *Na-alkaline complexes*: A, Cerro Patiño (39); B, Limpio (50); C, Cerro Verde (57, **61**); D, Ñemby (46, **61**); E, Cerro Confuso (55–61); F, Nueva Teblada (46–57); G, Lambaré (49); H, Tacumbú (41–46, **58**); I, Cerro Yariguaá (n.a.); J, Cerrito (**56**); K, Cerro Gimenez (66); L, Cerro Medina (n.a.); M, Colonia Vega (n.a.). Detailed information on the single occurrences, that is, geological map, location, country rocks, forms, and main rock-types, is provided in [33–36]; n.a.: not available.

segments (Figure 4): (1) the northwestern part, between the Asunción and Paraguarí townships, indicated also by the intragraben Ypacaray rifting and by the presence of Na-alkaline mafic-ultramafic plugs carrying mantle xenoliths (Asunción Province; age between 66 and 39 Ma; cf. Figure 4); (2) a central area, defined between Paraguarí and La Colmena townships, characterized by K-alkaline complexes and dykes (average age 127 Ma; cf. Figures 3 and 4) and by subordinate Na-alkaline complexes and dykes (age around 66–60 Ma); (3) the eastern part, between La Colmena and the Ybytyruzú hills, characterized by K-alkaline complexes and dykes (age around 130–125 Ma) and by tholeiitic lavas and flows (age around 133–130 Ma; cf. [4]).

Geology and gravity results indicate that the ASV graben extends up to 100 km into the Chaco Basin (Figures 2 and 3) and turns to an N80W trend between Paraguarí and Villarrica townships, in the area marked by a gravity low anomaly that increases eastwards (Figures 3 and 4). Paleomagnetic data [38] revealed that the potassic Cretaceous rocks (75 samples) have reversal polarity remnants corresponding to a paleomagnetic pole at 62.3°E and 85.4°S, similar to that calculated for the Serra Geral Formation in the Paraná Basin. It is therefore inferred that ASV K-alkaline rocks were emplaced, while the tholeiitic magmatic activity was still taking place (Figure 1).

Tertiary sodic rocks, carrying mantle xenoliths, mainly occur in an area characterized by relatively gravity highs (Figure 3), whereas the potassic complexes and dykes occur in a gravity low belt characterized by block faulting (Figures 3 and 4). Finally, an NS-trending fault system bounds the western side of the Ybytyruzú hills, close to several alkaline intrusions [24] East of Villarrica.

A total of 527 samples from the ASV area, including 220 dykes, have been investigated in detail, including field relationships, age, orientation (dykes), petrography, and mineral chemistry of the rocks reported in [10, 13, 33–36].

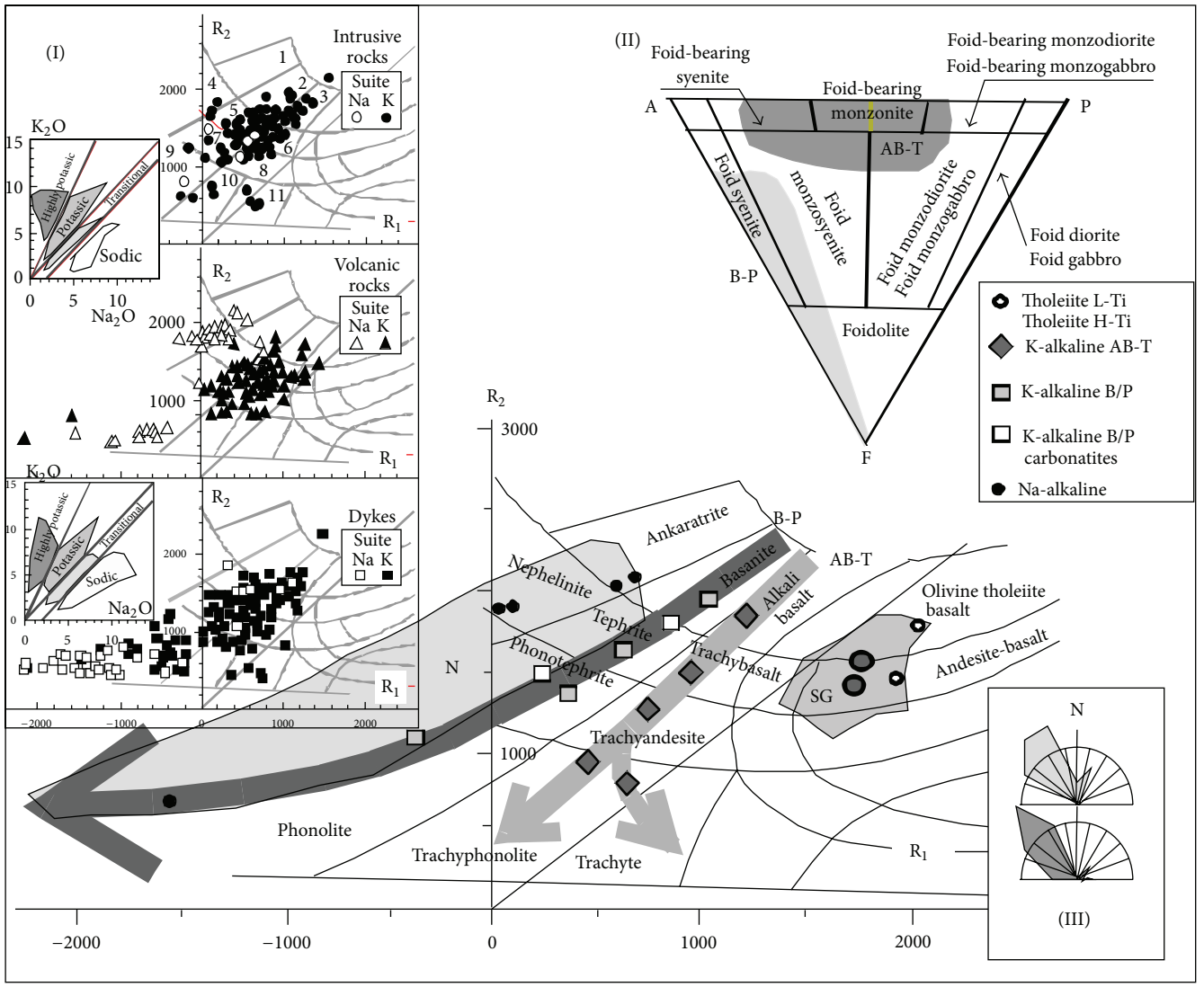

FIGURE 5: Compositional variation of the rock-types from ASV in terms of $R_1 = 4Si - 11(Na + K) - 2(Fe + Ti)$ and $R_2 = 6Ca + Mg + Al$ [39] (also Figure 2 of [13]). Data source: [34]. SG, field of Serra Geral tholeiites; ASV, field of Na-alkaline rocks; B-P and AB-T, lineages of the K-alkaline rocks (basanite to phonolitic suite and alkaline basalt to trachyphonolite/trachyte suite, resp.; white squares represent a lava flow and a theralite with carbonatitic affinity, resp. (see text)). Insets: (I), the same with subdivision into intrusive and volcanic rocks and dykes, plus Le Maitre [40] classification, as in Figure 2 of [10]. (II), QAPF diagram [41] for intrusive potassic suites from ASV, as from Figure 3 of [10]. (III), Azimutal frequence of the B-P and AB-T dykes [42]. The symbols represent selected compositions as in Tables 1 to 4.

55% of the dykes are preferentially oriented N20-60 W (Figure 5, (III)).

4. Classification, Petrography, and Petrochemistry of the Magmatic Rocks

The fine-grained texture of the ASV rocks, including the intrusive variants, is plotted on the De La Roche chemical classification [39] diagram (Figure 5), with an additional subdivision based on wt% K_2O and Na_2O on Le Maitre's [40] diagram (inset (I)).

4% of the dykes have tholeiitic affinity, sills, lava flows, and dykes, both high- and low-Ti variants, according to [2, 43] and straddle the fields of the olivine tholeiitic basalts and andesite-basalts, whereas 17% are sodic and 79% potassic in composition. The distribution of the potassic rocks shows that the variation of the dykes is consistent with that of the associated intrusive and volcanic rocks (inset (I)). Two main lineages are apparent for the potassic rock-types (Figure 5 and inset (II)): (1) a silica undersatured lineage (B-P) ranging from basanite to phonolite and peralkaline phonolite and (2) a silica-saturated lineage (AB-T) ranging from alkali basalt to trachyphonolite and trachyte [13, 42, 44].

In summary, tholeiitic rock-types (both high-titanium, H-Ti, and low-titanium, L-Ti, variants), K-alkaline, and Na-alkaline rocks are widespread in a relatively narrow area represented by ASV graben (ca. 35 × 200 km; cf. Figure 3). In Tables 1 to 4, representative and average analyses of these rocks are reported.

4.1. Tholeiites. The tholeiitic rocks are mainly lava flows (Ybytyruzú hills) and gabbro sills usually occurring near the Ybycuí township (Figure 4). The textures are porphyritic to aphanitic (lava flows and dykes) and equi- to subequigranular (sills), characterized by the presence of two clinopyroxenes (augite and pigeonite) and by pronounced variations of TiO_2 (1.4 to 3.2 wt%; cf. Table 1) and incompatible elements (IE: e.g., Ba ca. 150 to 400 ppm, Zr ca. 100 to 200 ppm). These variations are similar to those common to tholeiitic basalts of the Paraná Basin that are dominated by low and high contents of TiO_2 (L-Ti and H-Ti variants: southern and northern Paraná Basin with TiO_2 <2 and >2.5 wt%, resp.; cf. Figure 1) and IE [2, 45, 46]. The mineral assemblages (augite, pigeonite, olivine, plagioclase, magnetite, and ilmenite) show crystallization temperatures around 1200–1000°C and fO_2 conditions between NNO and QMF buffers [3].

Mass balance calculations and the remarkable differences in the ratios of the IE between L-Ti and H-Ti tholeiites suggest that such differences cannot be explained by fractional crystallization, or by means of melting and zone refining processes of a homogeneous mantle source. A basalt genesis from chemically different lithospheric mantle materials is therefore indicated. Mixing processes seem to have played a minor role [2, 47].

4.2. Potassic Suites. The different lithotypes of the potassic rocks (cf. Figure 5 and Tables 2 and 3) maybe subdivided into B-P and AB-T lineages, a distinction consistent with crystal fractionation models [13].

4.2.1. B-P Suite. The effusive rock-types and dykes (basanites, tephrites, and phonotephrites) typically show porphyritic textures with phenocrysts of clinopyroxene ($Wo_{40-50}Fs_{10-19}$), olivine (Fo_{60-85}), and leucite pseudomorphed by sanidine + nepheline in a glassy groundmass showing microlites of clinopyroxene ± olivine, Ti-magnetite ± ilmenite, Ti-phlogopite-biotite, alkali feldspar (Or_{15-88}), and nepheline-analcime ($Ne_{44-59}Ks_{17-26}$). Phenocrystal plagioclase (up to An_{74}) is also present. Accessory phases are amphibole (pargasite-kaersutite) and apatite ± zircon. Phonolites are characterized by phenocrysts of leucite-pseudomorphs, alkali feldspar (Or_{47-75}), clinopyroxene ($Wo_{48-50}Fs_{11-34}$), Fe-pargasite, and nepheline ± biotite ± titanite ± melanite (Ti-andradite up to 68 wt%) ± magnetite or haematite. Glassy groundmass contains microlites of alkali feldspar, nepheline, and clinopyroxene ± Ti-andradite ± magnetite. Haematite is found replacing magnetite or as a common groundmass constituent in peralkaline phonolites.

The intrusive analogues (theralites, essexitic gabbros, ijolites and essexites) show a holocrystalline inequigranular texture, with diopsidic pyroxene ($Wo_{44-51}Fs_{8-17}$), olivine (Fo_{75-82} to Fo_{44-66}), mica (Ti-phlogopite to Ti-biotite), Ti-magnetite, alkali feldspar, and nepheline ($Ne_{64-80}Ks_{20-36}$) ± leucite ± amphibole. "Intrusive" leucite and leucite pseudomorphed by analcime and plagioclase are common, testifying to subvolcanic conditions [24]. Cumulitic textures are represented by clinopyroxene with alkali feldspar + nepheline + carbonate as intercumulus phases.

On the whole, the temperatures calculated for the mineral assemblages span from 1250 to 1200°C and from 1130 to 1080°C, pheno- and microphenocrysts, respectively, under about 1 kb H_2O pressure and around 1000°C under atmospheric pressure; lower temperatures, for example, 900–700°C, suggest possible subsolidus exchange reactions (e.g., albitization). Magnetite-ilmenite pairs define temperatures between 1000 and 1100°C, along the NNO buffer [12].

Notably, the B-P suite is also characterized by carbonatitic magmatism, although it is very limited in volume. A silicobeforsitic flow is present in the Sapucai lava sequences and as "ocelli" at the Canãda and Cerro E. Santa Helena K-alkaline complexes [48]. These primary carbonates are relevant as they reveal a CO_2 imprinting after the tholeiitic magmatism.

4.2.2. AB-T Suite. Alkali gabbros, syenogabbros, and syenodiorites are usually porphyritic and seriate in texture. They contain clinopyroxene ($Wo_{43-50}Fs_{6-14}$), olivine (Fo_{43-82}), Ti-biotite, Ti-magnetite ± ilmenite, plagioclase (An_{31-78}), alkali feldspar (Or_{60-84}), interstitial nepheline-analcime ($Ne_{37-82}Ks_{15-23}$), and alkali feldspar (Or_{80-97}). Accessories are apatite ± amphibole ± titanite ± zircon. Nepheline syenites and syenites are texturally equi- to subequigranular and seriate. The rock-types are characterized by alkali feldspar (Or_{32-63}), clinopyroxene ($Wo_{43-48}Fs_{10-32}$), and nepheline (Ne_{85}) and hastingsite. Common accessories include titanite and apatite ± carbonate ± zircon.

Alkali basalts, trachybasalts, and trachyandesites are porphyritic rocks exhibiting phenocrysts and/or microphenocrysts of clinopyroxene ($Wo_{44-49}Fs_{7-15}$), olivine (Fo_{65-83}), plagioclase (An_{28-76}), magnetite, and biotite set in a glassy groundmasses consisting of microlites of clinopyroxene ($Wo_{46-49}Fs_{13-18}$), magnetite, ilmenite, biotite, plagioclase (An_{20-45}), alkali feldspar (Or_{52-65}), nepheline-analcime ($Ne_{37-73}Ks_{22-38}$), amphibole, and apatite ± titanite ± zircon.

Trachyphonolites and trachytes are porphyritic to aphyric. The phenocrysts are alkali feldspar (Or_{60-65}) ± clinopyroxene ($Wo_{46-49}Fs_{14-20}$) ± plagioclase (An_{14-16}), pseudomorphosed leucite, amphibole, and biotite in a hypocrystalline to glassy groundmass containing microlites of alkali feldspar, biotite, and clinopyroxene ± biotite ± amphibole ± magnetite ± Ti-andradite ± haematite.

Notably, the equilibration temperatures of the mineral assemblages are very similar to those suggested for the B-P suite [10, 13, 49].

The differentiation history of the potassic ASV magmas remained largely into the stability fields of the ferromagnesian phases [12], that is, olivine + clinopyroxene, in the system Mg_2SiO_4-$KAlSiO_4$ [10, 13, 51], suggesting that relatively high temperature subvolcanic conditions were prevalent. Moreover, the extreme differentiates from both B-P and AB-T suites approaches to the composition of peralkaline residua, pointing to an extensive subvolcanic crystallization of K-rich, aluminous phases, likely phlogopite and leucite, at least for the B-P suite [52].

Table 1: Averages of representative chemical analyses (recalculated to 100 wt% on anhydrous basis; in parentheses, standard deviation) of tholeiites from ASV [33, 34, 44]. L-Ti and H-Ti tholeiites according to [2, 45]. The ε time-integrated notations are calculated using the present day Bulk Earth parameters [50], that is, UR = 0.7047 ($^{87}Rb/^{86}Sr = 0.0816$) and CHUR = 0.512638 ($^{147}Sm/^{144}Nd = 0.1967$. Mg#: molar ratio MgO/(MgO + FeO)).

Suite: tholeiite	L-Ti basalt	L-Ti andesite-basalt	H-Ti basalt	H-Ti Andesite-basalt
No. of samples	(3)	(3)	(6)	(5)
Wt%				
SiO_2	50.20 (0.79)	53.06 (0.40)	50.83 (0.84)	50.52 (0.60)
TiO_2	1.40 (0.06)	1.36 (0.11)	2.58 (0.36)	3.19 (0.60)
Al_2O_3	14.64 (0.21)	13.78 (0.09)	13.98 (0.45)	14.25 (0.63)
FeO_{tot}	12.73 (0.39)	13.42 (0.49)	13.54 (0.56)	14.55 (1.13)
MnO	0.19 (0.05)	0.25 (0.05)	0.21 (0.02)	0.21 (0.02)
MgO	7.36 (0.22)	5.53 (0.08)	5.13 (0.44)	4.19 (0.65)
CaO	10.63 (0.66)	8.55 (0.05)	9.65 (0.62)	8.56 (0.44)
Na_2O	2.36 (0.11)	2.66 (0.20)	2.61 (0.15)	2.49 (0.29)
K_2O	0.33 (0.05)	1.07 (0.18)	1.10 (0.17)	1.14 (0.10)
P_2O_5	0.15 (0.02)	0.19 (0.01)	0.37 (0.09)	0.36 (0.04)
Mg#	0.66	0.55	0.54	0.48
ppm				
La	6.2 (0.8)	9.0 (1.0)	25.3 (6.3)	26.0 (6.0)
Ce	16.0 (1.7)	21.0 (2.9)	60.4 (12.2)	50.0 (2.0)
Nd	11.1 (1.3)	14.1 (2.2)	28.3 (3.6)	25.0 (3.0)
Sm	3.4 (0.3)	4.3 (0.4)	7.7 (1.5)	6.8 (1.1)
Eu	1.2 (0.1)	1.5 (0.1)	2.2 (0.2)	1.9 (0.2)
Gd	4.3 (0.6)	5.4 (0.8)	7.7 (1.2)	6.9 (1.1)
Dy	4.8 (0.5)	6.0 (0.9)	6.3 (1.5)	5.7 (1.3)
Er	2.9 (0.4)	3.6 (0.6)	3.9 (1.3)	3.5 (0.9)
Yb	2.6 (0.4)	3.2 (0.4)	3.4 (1.2)	3.2 (1.0)
Lu	0.34 (0.07)	0.42 (0.09)	0.49 (0.15)	0.50 (0.19)
Cr	325 (27)	62 (1)	119 (15)	48 (2)
Ni	103 (18)	55 (7)	60 (15)	54 (12)
Rb	13 (4)	13 (1)	24 (3)	33 (11)
Sr	188 (42)	187 (2)	386 (90)	334 (15)
Ba	154 (19)	190 (4)	409 (78)	347 (37)
Th	1.1 (0.1)	1.7 (0.2)	2.0 (0.1)	3.0 (0.2)
U	0.24 (0.05)	0.37 (0.08)	0.43 (0.08)	0.65 (0.04)
Ta	0.28 (0.04)	0.42 (0.07)	1.2 (0.3)	1.8 (0.4)
Nb	4.0 (1.0)	6.1 (1.0)	13 (2)	20 (1)
Zr	83 (10)	113 (2)	190 (36)	197 (6)
Y	28 (2)	42 (1)	33 (4)	36 (3)
Measured				
($^{87}Sr/^{86}Sr$)	0.70548 (20)	0.70535 (20)	0.70617 (21)	0.70620 (18)
($^{143}Nd/^{144}Nd$)	0.51271 (9)	0.51272 (10)	0.51239 (2)	0.51240 (1)
Age (Ma): 131.6				
Initial ratio				
$(^{87}Sr/^{86}Sr)_i$	0.70502	0.70456	0.70576	0.70554
$(^{143}Nd/^{144}Nd)_i$	0.51256	0.51256	0.51225	0.51226
T_{DM}	1991	1976	2127	2037
R_1	2037	1929	1758	1722
R_2	1789	1459	1561	1403
εSr	6.70	0.12	17.16	14.12
εNd	1.60	1.79	−4.30	−4.10

4.3. The Sodic Rocks. These consist mainly of ankaratrites + (mela)nephelinites (45%) and phonolites (42%) (Comin-Chiaramonti et al. [10, 13, 44]). Representative chemical analyses are reported in Table 4.

Phenocrysts-microphenocrysts in ankaratrites and nephelinites are characterized by olivine (phenocrysts 1–7 vol%, Fo_{89-85} mole%; 1–6 vol% microphenocrysts, Fo_{82-77} mole%), clinopyroxene (phenocrysts 1–6 vol%, Mg# ~0.8), titanomagnetite (0.3–0.7 vol%, up to 38 ulv. mole%), and occasionally phlogopite microphenocrysts. The hypocrystalline groundmass contains clinopyroxene (39–46 vol%, Mg# ~0.75), olivine (3–6 vol%, Fo_{74-76} mole%), titanomagnetite (4–7 vol%, up to 43% ulv. mole%), nepheline (16–21 vol%), and glass (11–25 vol%) [53].

Phonolites are typically microphyric to hypocrystalline with alkali feldspar phenocrysts or microphenocrysts (Or_{43-83}), nepheline (Ne_{67-79}), occasionally altered to cancrinite, acmitic clinopyroxene (acmite up to 63 wt%), and ferroedenite-ferropargasite amphibole. Haüyne, mica, haematite, and zircon are typical accessory minerals. Analcime occurs as a nepheline pseudomorph. Ti-andradite and titanite phenomicrophenocrysts are present in some dykes [10].

Lherzolite, harzburgite, dunite mantle xenoliths, and xenocrystic debris are common and abundant in the ankaratrites and nephelinites [54] from eastern ASV (Figure 3).

The generation of the ASV nephelinites may be modelled for 4–6% degrees of partial melting, with crystallization temperatures between 1200 and 1000°C from garnet peridotite sources [10, 55].

4.4. Mantle Xenoliths. The xenoliths are mainly spinel-lherzolites, harzburgites, and subordinate dunites. The dominant texture is protogranular, rarely tabular or porphyroclastic [54]. The Paraguay mantle xenoliths contain variable amounts of glassy patches (blebs) and glassy drops in clinopyroxenes [56]. The latter show an overprinted spongy texture [54]. The blebs (whole composition: Mg# 0.88–0.91) consist mainly of a glassy matrix having microlites of olivine (Mg# 0.91-0.92), clinopyroxene (Mg# 0.91–0.93), Cr-spinel, and (rarely) phlogopite (Mg# 0.86–0.92). According to [56, 57], they were formed by decompression melting of amphibole and phlogopite.

The Paraguayan xenoliths are characterized by a large range of K_2O (0.02 to 0.51 wt%). Some xenoliths have K_2O abundances comparable or even higher than those reported for metasomatized mantle peridotites [58], resembling in some cases to amphibole-mica-apatite-bearing mantle-xenolith suites [59]. K_2O contents and the abundance of blebs and glassy drops allow to group the Paraguay xenoliths into two main suites, that is, a low-K suite (LK, K_2O <0.15 wt%) and a high-K suite, the latter with abundant glassy drops and/or variable amounts of blebs and spongy clinopyroxenes (HK, K_2O ≥0.2 wt%). Representative analyses are listed in Table 5, and complete sets of chemical analyses are in [54].

Based on Spera's [60] approach, Comin-Chiaramonti et al. [55] suggested that the ascent of the xenoliths to the surface took place in a very short time, for example, less than nine days (assuming a diameter of 45 cm, corresponding to the largest xenolith size, a density of 3.3 g/cm^3, and an origin of the hosting liquids from depth ~70–75 km, i.e., ~boundary between garnet and spinel peridotite). These mantle xenoliths provide a direct sampling of the subcontinental mantle in ASV along with the metasomatic processes [61, 62].

Coherent variations of major element in both suites follow a dunite-lherzolite sequence trending to the mantle composition [54]. The population is represented mainly by lherzolitic-harzburgitic (dunitic) compositions, mostly with a 0.55–0.63 range of $(SiO_2 + Al_2O_3)/(MgO + FeO_t)$ molar ratio. The residual character of the harzburgitic mantle xenoliths (believed to be consistent with melting and basalt-component removal) is also indicated by the decrease in the cpx/opx modal ratio with decreasing modal cpx, which fits the model variation trend induced by partial melting of lherzolite [56, 63].

Equilibration temperatures for orthopyroxene-clinopyroxene pairs [64] and for olivine-spinel pairs [65] vary between 862° and 1075°C and between 748° and 968°C, respectively. Intracrystalline temperatures [66–68] for clinopyroxene and orthopyroxene pairs vary between 936° and 1033°C and between 920 and 1120°C (LK and HK suites, resp., with pressures in the range of 1.1–2.3 GPa for both suites, with the higher values related to the more depleted xenoliths from the LK suite [53, 56]).

The oxygen isotope compositions on separates of clinopyroxene and coexisting olivine ($\delta^{18}O‰$) vary from 5.5 to 6.0‰and from 5.0 to 6.1‰, respectively [53]. These isotopic ratios are in the range for worldwide mantle phases: olivine, 4.4 to 7.5‰, and clinopyroxene, 4.8 to 6.7‰ [69, 70], and for South America mantle xenoliths: olivine, 4.9 to 6.4‰, and clinopyroxene, 5.0 to 6.0‰ [71]. The calculated Cpx-Ol isotopic temperatures [53, 71] are around 970–1070°C, 1030–1130°C (LK), and 1100–1180°C (HK), suggesting equilibration temperatures higher in the HK suite than in LK suite.

The highest temperature of the HK suite is substantially due to higher $\delta^{18}O‰$ in olivine than $\delta^{18}O‰$ in clinopyroxene. According to [72], the relatively low $\delta^{18}O$ in the pyroxenes reflects metasomatism by a silicate melt from subducted altered oceanic crust. Therefore, the Paraguayan HK suite would be for some geologists the best candidate for a subduction-related environment.

Notably, the ASV clinopyroxenes [73] have V_{Cell} and V_{M1} sites intermediate between those of plagioclase- and garnet-bearing mantle peridotites, that is, in a pressure range between 1.2 and 2.2 GPa. Thus, isotopic and crystallographic results are internally consistent.

On the whole, the ASV xenoliths define a geotherm [53] which, starting at about 830°C and 1.0 GPa, at the transition mantle-crust, intersects the hydrous peridotite solidus at about 1140°C and 2.1-2.2 GPa in the spinel peridotite facies, near to the transition with the garnet peridotite facies, believed to be the source of the sodic alkaline magmatism.

5. Geochemistry

Incompatible elements (i.e., large ion lithophile elements, IE, LILE, and high field strength elements (HFSE)),

Table 2: Representative chemical analyses (recalculated to 100 wt% on anhydrous basis; in parentheses, standard deviation) of K-alkaline rocks (B-P suite, effusive and intrusive equivalents and dykes) from ASV [10, 13, 24]. Analysis of a silicobeforsitic flow, on anhydrous basis, is also shown [48, 74]. Ages as in [4].

Suite B-P						
K-alkaline	Basanite	Tephrite	Phonotephrite	Phonolite	Silicobeforsite 22% dolomite	Silicobeforsite carb. fraction
No. of samples	(4)	(6)	(4)	(1)	(1)	
Wt%						
SiO_2	46.95 (2.14)	49.08 (1.31)	52.36 (1.64)	48.69	49.05	—
TiO_2	1.78 (0.19)	1.94 (0.26)	1.42 (0.19)	1.97	1.94	—
Al_2O_3	12.84 (1.63)	12.94 (1.17)	17.27 (1.24)	16.42	15.32	—
FeO_{tot}	10.20 (1.80)	10.02 (0.97)	7.39 (0.75)	8.45	9.60	—
MnO	0.18 (0.03)	0.17 (0.02)	0.15 (0.02)	0.15	0.17	—
MgO	9.95 (2.02)	7.88 (1.64)	3.66 (0.58)	3.86	5.28	—
CaO	11.31 (1.41)	9.36 (0.85)	7.00 (1.02)	6.96	8.81	—
Na_2O	2.42 (0.61)	2.99 (0.92)	4.34 (0.58)	3.79	3.50	—
K_2O	3.78 (1.18)	4.99 (1.24)	5.73 (0.17)	8.60	6.14	—
P_2O_5	0.59 (0.21)	0.66 (0.18)	0.58 (0.07)	0.69	0.34	—
Mg#	0.67	0.62	0.51	0.45	—	—
ppm						
La	82.1 (19.0)	91.2 (13.0)	93.3 (13.6)	98	80	239.06
Ce	162.6 (30.4)	164.1 (18.1)	170.0 (25.0)	186	145	420.34
Nd	64.4 (10.9)	69.3 (4.9)	66.6 (12.1)	73.2	62	159.89
Sm	12.8 (2.4)	12.8 (3.6)	11.4 (1.6)	15.1	11.3	19.06
Eu	3.0 (0.6)	3.0 (0.4)	2.8 (0.3)	2.02	2.3	3.90
Gd	7.4 (1.9)	6.8 (1.1)	7.1 (0.6)	5.93	8.8	14.90
Dy	4.4 (0.6)	3.6 (0.2)	3.9 (0.4)	2.86	6.2	10.57
Er	1.9 (0.4)	1.7 (0.3)	1.9 (0.3)	1.59	3.3	5.40
Yb	1.6 (0.1)	1.4 (0.4)	1.5 (0.3)	1.59	1.9	3.16
Lu	0.25 (0.01)	0.21 (0.06)	0.26 (0.06)	0.23	0.28	0.32
Cr	275 (106)	378 (260)	36 (23)	53	51	—
Ni	81 (29)	111 (42)	28 (18)	22	18	—
Rb	88 (18)	117 (51)	111 (35)	260	148	0.21
Sr	1134 (279)	1661 (227)	1569 (10)	1626	1126	268
Ba	1179 (252)	1582 (147)	1462 (215)	1935	1350	—
Th	14.4 (9.9)	11.4 (3.5)	12.1 (1.6)	12.7	15.2	—
U	2.9 (1.0)	2.4 (0.7)	2.5 (0.1)	3.5	4.2	—
Ta	3.2 (0.2)	3.0 (0.7)	3.2 (0.3)	5.1	2.7	—
Nb	38.0 (7.0)	44 (10)	47 (1)	62	35	—
Zr	246 (42)	282 (91)	259 (35)	365	280	—
Y	14.0 (2.8)	17.3 (6.7)	18.9 (3.0)	13	18	23.75
Measured						
$(^{87}Sr/^{86}Sr)$	0.70761 (4)	0.70774 (3)	0.70727 (4)	0.70752 (2)	0.70807 (2)	0.70762 (3)
$(^{143}Nd/^{144}Nd)$	0.51182 (4)	0.51171 (1)	0.51160 (4)	0.51187 (2)	0.511804 (6)	0.511371 (8)
Age	130	129	124	125	128	—
Initial ratio						
$(^{87}Sr/^{86}Sr)_i$	0.70697	0.70716	0.70671	0.70645	0.70700	0.70717
$(^{143}Nd/^{144}Nd)_i$	0.51172	0.51162	0.51152	0.51177	0.51171	0.51131
T_{DM}	2049	2042	2043	2067	1884	1844
R_1	1054	713	365	−397	—	—
R_2	1955	1646	1269	1258	—	—
εSr	34.31	37.04	30.58	26.88	34.7	34.17
εNd	−14.69	−16.71	−18.78	−13.83	−14.8	−22.7

Table 3: Representative chemical analyses (recalculated to 100 wt% on anhydrous basis; in parentheses, standard deviation) of K-alkaline rocks (AB-T suite, effusive and intrusive equivalents and dykes) from ASV [13, 74]. Ages as in [4].

Suite AB-T					
K-alkaline	Alkaline basalt	Trachybasalt	Trachyandesite	Trachyphonolite	Trachyte
No. of samples	(3)	(3)	(7)	(5)	(1)
Wt%					
SiO_2	48.69 (1.50)	50.90 (1.56)	53.16 (1.18)	58.25 (1.44)	58.95
TiO_2	1.69 (0.48)	1.49 (0.31)	1.42 (0.21)	0.91 (0.23)	1.94
Al_2O_3	15.17 (1.86)	17.07 (1.06)	16.99 (1.45)	18.39 (1.01)	19.03
FeO_{tot}	10.31 (0.76)	9.04 (0.57)	7.96 (0.75)	4.87 (1.51)	4.49
MnO	0.19 (0.01)	0.16 (0.02)	0.15 (0.02)	0.16 (0.01)	0.12
MgO	6.71 (0.89)	5.01 (0.24)	4.03 (0.58)	0.89 (0.90)	1.69
CaO	11.09 (0.63)	8.58 (1.11)	6.95 (0.66)	4.59 (1.09)	3.37
Na_2O	3.16 (0.42)	3.64 (0.44)	4.10 (0.38)	5.89 (1.38)	4.21
K_2O	2.46 (0.42)	3.65 (0.72)	4.61 (1.06)	5.76 (1.13)	7.00
P_2O_5	0.55 (0.36)	0.50 (0.17)	0.55 (0.09)	0.29 (0.10)	0.25
Mg#	0.58	0.53	0.51	0.32	0.40
ppm					
La	51.2 (16.0)	54.0 (18.6)	82.8 (29.7)	154.0 (33.9)	136
Ce	106.7 (24.4)	109.0 (21.0)	154.2 (55.7)	261.1 (44.2)	206
Nd	52.7 (19.7)	47.9 (12.9)	64.7 (15.7)	84.0 (17.7)	78
Sm	10.5 (1.6)	9.4 (30.5)	10.8 (2.1)	12.7 (3.5)	15.1
Eu	2.8 (1.0)	2.5 (0.3)	2.8 (0.5)	3.28 (0.8)	3.9
Gd	6.8 (2.4)	6.0 (1.2)	6.4 (1.0)	5.70 (1.6)	9.4
Dy	4.1 (0.7)	4.2 (0.6)	4.2 (0.7)	5.44 (1.1)	6.3
Er	1.7 (0.1)	1.8 (0.3)	1.6 (0.4)	2.59 (0.58)	2.3
Yb	1.5 (0.1)	1.6 (0.4)	1.6 (0.4)	2.25 (0.46)	2.0
Lu	0.22 (0.05)	0.24 (0.03)	0.28 (0.08)	0.35 (0.08)	0.31
Cr	143 (24)	92 (59)	38 (34)	10 (6)	8
Ni	49 (6)	31 (18)	17 (12)	6 (2)	2
Rb	53 (13)	98 (16)	87 (20)	7 (3)	133
Sr	1573 (263)	1389 (407)	1474 (194)	77 (34)	600
Ba	1033 (321)	1280 (170)	1211 (168)	1377 (215)	1726
Th	4.3 (2.1)	7.9 (1.5)	14.6 (8.5)	31.7 (8.5)	—
U	1.3 (0.5)	1.7 (0.6)	3.4 (3.0)	9.5 (3.3)	—
Ta	2.3 (1.1)	1.6 (0.4)	2.8 (0.7)	2.6 (0.6)	2.5
Nb	18.1 (9.0)	25.0 (6.0)	40 (12)	62 (18)	61
Zr	260 (31)	220 (33)	268 (14)	411 (128)	392
Y	14.5 (9.2)	14.6 (6.5)	19.5 (3.2)	25 (4)	23
Measured					
$(^{87}Sr/^{86}Sr)$	0.70717 (4)	0.70721 (5)	0.70753 (4)	0.70752 (2)	0.70807 (2)
$(^{143}Nd/^{144}Nd)$	0.51185 (4)	0.51170 (3)	0.51160 (4)	0.51187 (2)	0.51181 (6)
Age	125	119	129	125	128
Initial ratio					
$(^{87}Sr/^{86}Sr)_i$	0.70693	0.70673	0.70709	0.70708	0.70639
$(^{143}Nd/^{144}Nd)_i$	0.51175	0.51161	0.51151	0.51179	0.51171
T_{DM}	2009	2199	1999	1530	2001
R_1	1215	954	749	545	649
R_2	1817	1501	1277	1014	818
εSr	33.68	30.74	36.09	35.85	26.0
εNd	−14.16	−17.12	−18.68	−13.31	−14.9

Table 4: Representative chemical analyses (recalculated to 100 wt% on anhydrous basis; in parentheses, standard deviation) of Na-alkaline rocks from ASV ASV [13, 74]. Ages as in [4].

Suite: sodic Na-Alkaline	Ankaratrite	Ankaratrite	Ankaratrite	Melanephelinite	Peralkaline Phonolite
No. of samples	(1)	(1)	(5)	(1)	(1)
Wt%					
SiO_2	43.71	43.97	43.29 (0.65)	45.67	55.96
TiO_2	2.39	2.12	2.50 (0.48)	2.21	0.43
Al_2O_3	14.84	13.87	13.42 (0.95)	14.83	21.19
FeO_{tot}	10.01	10.44	10.71 (0.40)	7.83	4.04
MnO	0.18	0.21	0.19 (0.01)	0.20	0.22
MgO	10.07	9.87	11.47 (1.23)	8.92	0.21
CaO	12.06	10.81	11.82 (0.28)	10.78	1.34
Na_2O	5.15	6.00	4.12 (0.21)	6.73	10.77
K_2O	0.89	1.51	1.61 (0.32)	1.54	5.76
P_2O_5	0.90	1.22	0.88 (0.14)	1.28	0.08
Mg#	0.74	0.72	0.69	0.58	0.22
ppm					
La	81	119	84.2 (12.4)	118	120
Ce	145	186	162.8 (24.3)	190	191
Nd	43.4	63.7	55.2 (8.5)	65.1	65
Sm	8.15	11.23	9.4 (1.2)	11.45	11
Eu	1.89	2.15	2.7 (0.3)	2.18	—
Gd	5.77	5.16	6.7 (0.7)	5.23	—
Dy	4.81	4.81	5.5 (0.7)	5.00	—
Er	2.13	2.75	2.4 (0.3)	2.86	—
Yb	1.65	1.79	1.8 (0.3)	1.87	—
Lu	0.23	0.27	0.27 (0.04)	0.28	—
Cr	542	648	490 (74)	470	2
Ni	207	273	249 (48)	239	6
Rb	22	59	53 (13)	63	60
Sr	1016	1013	1109 (63)	1095	654
Ba	1090	980	1090 (95)	1094	367
Th	10.5	10.5	11.0 (2.4)	11.6	—
U	2.3	2.3	2.4 (0.5)	2.5	—
Ta	5.9	5.9	8.4 (1.0)	6.5	—
Nb	86	101	105 (13)	113	—
Zr	152	234	250 (43)	228	955
Y	26	33	29 (4)	32	39
Measured					
$(^{87}Sr/^{86}Sr)$	0.70395 (1)	0.70374 (1)	0.70381 (8)	0.70392 (1)	0.70405 (2)
$(^{143}Nd/^{144}Nd)$	0.51275 (1)	0.51276 (1)	0.512724 (61)	0.51274 (2)	0.51268 (2)
Age	46	46	46	50	60
Initial ratio					
$(^{87}Sr/^{86}Sr)_i$	0.70391	0.70364	0.70373	0.70381	0.70384
$(^{143}Nd/^{144}Nd)_i$	0.51272	0.51273	0.51269	0.51271	0.51264
T_{DM}	581	532	562	558	617
R_1	582	100	682	18	−1567
R_2	2080	1918	2096	1886	570
εSr	−10.42	−14.30	−13.05	−11.79	−11.19
εNd	2.67	2.91	2.23	2.57	1.54

Table 5: Average chemical analyses (recalculated to 100 wt% on anhydrous basis; in parentheses, standard deviation) of mantle xenoliths (LK and HK suites, K_2O <0.15 wt%, and >0.2 wt%, resp.from ASV [53, 54, 56]. The age is the average of ages of Table 4. The bleb is a representative glassy drop in an H-K harzburgite [54, 56].

Whol-rock	L-K lherzolite	L-K harzburgite	H-K lherzolite	H-K harzburgite	H-K bleb
No. of samples	(5)	(6)	(3)	(2)	(1)
Wt%					
SiO_2	44.02 (1.15)	43.95 (0.35)	44.65 (0.11)	44.63 (0.20)	46.15
TiO_2	0.03 (0.02)	0.01 (0.00)	0.07 (0.03)	0.02 (0.00)	0.70
Al_2O_3	1.76 (0.86)	1.14 (0.50)	2.37 (0.04)	1.36 (0.03)	10.10
FeO_{tot}	7.97 (0.13)	7.85 (0.22)	7.92 (0.24)	7.52 (0.01)	6.74
MnO	0.12 (0.01)	0.11 (0.00)	0.11 (0.01)	0.11 (0.00)	0.14
MgO	44.17 (1.87)	45.58 (1.60)	41.55 (0.46)	44.76 (0.21)	23.67
CaO	1.75 (0.86)	1.18 (0.69)	2.64 (0.23)	1.12 (0.02)	6.56
Na_2O	0.12 (0.01)	0.10 (0.05)	0.28 (0.01)	0.16 (0.01)	2.00
K_2O	0.09 (0.04)	0.06 (0.04)	0.39 (0.10)	0.32 (0.00)	3.10
P_2O_5	0.21 (0.10)	0.01 (0.01)	0.01 (0.00)	0.02 (0.00)	0.83
ppm					
La	1.69 (0.12)	2.87 (0.51)	2.66 (0.52)	6.71 (0.69)	77.39
Ce	1.53 (0.09)	4.09 (0.75)	3.35 (0.67)	8.45 (0.81)	106.25
Nd	0.20 (0.01)	0.28 (0.16)	0.96 (0.55)	2.42 (0.25)	27.74
Sm	0.012 (0.004)	0.038 (0.015)	0.260 (0.014)	0.51 (0.20)	4.16
Eu	0.001 (0.001)	0.006 (0.002)	0.010 (0.01)	0.020 (0.006)	1.00
Gd	0.07 (0.008)	0.04 (0.01)	0.37 (0.02)	0.74 (0.03)	2.92
Dy	0.10 (0.01)	0.05 (0.01)	0.43 (0.02)	0.91 (0.04)	2.61
Er	0.07 (0.001)	0.05 (0.01)	0.30 (0.01)	0.65 (0.06)	1.68
Yb	0.07 (0.001)	0.08 (0.01)	0.29 (0.01)	0.63 (0.03)	1.23
Lu	—	—	—	—	
Cr	2601 (350)	2421 (357)	2360 (88)	2635 (30)	38114
Ni	2307 (160)	2309 (102)	2120 (4)	2307 (73)	1124
Rb	3.33 (9.51)	2.67 (1.63)	7.50 (2.12)	6.00 (1.41)	120
Sr	22.41 (10.47)	11.15 (4.58)	28.89 (10.29)	64.67 (7.62)	1414
Ba	20.0 (10.0)	4.67 (1.18)	40 (8)	34.5 (14.8)	1781
Th	—	—	—	—	—
U	—	—	—	—	—
Ta	—		—	—	—
Nb	5.91 (0.58)	1.78 (0.20)	6.39 (1.77)	6.98 (1.01)	155
Zr	5.95 (0.41)	6.08 (0.45)	6.90 (0.13)	7.86 (0.93)	189
Y	0.51 (0.10)	0.72 (0.09)	2.62 (0.09)	5.70 (1.08)	14.70
Measured					
$(^{87}Sr/^{86}Sr)$	0.70426 (0.00005)	0.70421 (0.00038)	0.70416 (0.00006)	0.70395 (0.00002)	—
$(^{143}Nd/^{144}Nd)$	0.51264 (0.00007)	0.51275 (0.00039)	0.51299 (0.00033)	0.51288 (0.00005)	—
Age	(50 ± 6)	(50 ± 6)	(50 ± 6)	(50 ± 6)	—
Initial ratio					
$(^{87}Sr/^{86}Sr)_i$	0.70398	0.70376	0.70367	0.70377	—
$(^{143}Nd/^{144}Nd)_i$	0.51263	0.51272	0.51294	0.51285	—
T_{DM}	427	448	446	453	—
εSr	−9.40	−12.55	−13.80	−12.31	—
εNd	1.06	2.92	7.08	5.16	—

considered with the Sr-Nd isotopic composition, indicate that the ASV magmatic was generated from geochemically distinct (enriched versus depleted) mantle sources (cf. [75]).

5.1. Incompatible Elements. Mantle-normalized IE patterns for the various and different magmatic rock groups are represented in Figure 6.

The L-Ti and H-Ti ASV tholeiites are distinct in terms of their relatively low elemental abundances and high LILE/HFSE ratios. In particular, their marked Ta-Nb negative spikes are similar to those of the potassic alkaline magmas from ASV, but clearly different in comparison to the Cenozoic sodic alkaline rocks from the same area.

The suites are similarly enriched in REE and exhibit steep, subparallel LREE trends ($(La/Lu)_{CN}$ = 26–161, 17–62 and 11–46 for B-P, AB-T and Na rocks, resp.), which tend to flatten out for HREE ($(Dy/Lu)_{CN}$ = 1.24–1.96, 1.09–2.00 and 0.56–2.05 for B-P, AB-T and Na rocks, resp.); HK-dykes are excepted. REE profiles with LREE enrichment and flat HREE suggest mantle sources previously depleted by melt extraction and subsequently enriched [76].

Multielemental diagrams, normalized to a primordial mantle composition (Figure 6) show a substantial overlap of B-P and AB-T compositions, negative Nb, Ta, P, Ti, and Y spikes, and positive U, K, and Sr anomalies. In general, B-P compositions are higher in Rb, K, Zr, Hf, Ti, Y, LREE, and MREE than AB-T compositions. On the contrary, the Na rocks yielded La/Nb and La/Ta ratios close to unity, respectively, and Nb/K and Ta/K ratios greater than 1.0, respectively. Notably, the variations of incompatible elements of the AB-T compositions mimic to some extent those of the ASV H-Ti (and L-Ti) tholeiitic basalts, which approach the lower (Rb to Nd) and higher (Sm to Lu) elemental concentrations of that suite (Figure 6).

In summary, substantial overlap in bulk-rock chemistry exists between the investigated B-P and AB-T rocks, both characterized by variable K/Na ratio, the K types being dominant. REE and other incompatible elements show similar concentration levels and variation trends in the two suites. The mantle normalized incompatible element patterns of both ASV suites show strong affinities, including negative "Ta-Nb-Ti anomalies," with the Paraná tholeiites [10].

On the whole, the geochemical features suggest that the enrichment processes were related to small-volume melts in a lithospheric mantle [4, 10, 74].

5.2. Sr-Nd Isotopes. The investigated rocks from ASV show a large distribution of Sr-Nd isotopic compositions (Figure 7), delineating a trend similar to the "low Nd" array of [77] (cf. also "Paraguay array" of [4]). Due to the high Sr and Nd of the most "primitive" alkaline rocks and associated carbonatites from Eastern Paraguay, Comin-Chiaramonti et al. [12] suggested that initial Sr-Nd isotopic ratios of these rocks can be considered uncontaminated by the crust and, as a result, representative of the isotopic composition of their mantle source(s). The ASV potassic rocks have the highest (time integrated) Sr_i and the lowest Nd_i. Including the carbonatites of the BP-suite [24, 78], the Sr_i and Nd_i range from 0.70645 to 0.70716 and from 0.51151 to 0.51179, respectively (Tables 2 and 3). These values are quite distinct from those of the ASV Paleocene sodic rocks (ca. 60 Ma), which plot within the depleted quadrant (Sr_i = 0.70364–0.70391, Nd_i = 0.51264–0.51273; cf. Table 4), towards the HIMU-DMM depleted mantle components (Figure 7). Notably, Sr_i and Nd_i of the tholeiites, believed to be uncontaminated [10], both H- and L-Ti, are intermediate between the potassic and sodic rocks: 0.70456–0.70576 and 0.51225–0.51256, respectively (cf. Table 4). These values approach to the range of the Early Cretaceous uncontaminated tholeiites from the Paraná Basin [47], that is, Sr_i = 0.70527 ± 0.00051 and Nd_i = 0.51264 ± 0.00011. To be stressed that the genesis of these tholeiites requires lithospheric mantle components, as indicated by K-alkaline and carbonatitic rocks from ASV [4, 5].

Considering the whole Paraná-Agola-Etendeka system (PAE), and that the ASV is located at the central westernmost side of the PAE [5, 6], the different geochemical behaviour in the different PAE sectors implies also different sources. Utilizing the T_{DM} (Nd) model ages [78, 79], it should be noted that (1) the H-Ti flood tholeiites and dyke swarms from the Paraná Basin and the Early Cretaceous potassic rocks and carbonatites from Eastern Paraguay range mainly from 0.9 to 2.1 Ga, whereas in Angola and Namibia the Early Cretaceous K-alkaline rocks vary from 0.4 to 0.9 Ga; (2) the L-Ti tholeiites display a major T_{DM} variation, from 0.7 to 2.4 Ga (mean 1.6 ± 0.3) with an increase of the model ages from North to South; (3) Late Cretaceous alkaline rocks show model ages ranging from 0.6 to 1 Ga, similar to the age span shown by the Triassic to Paleocene sodic alkaline rock-types lying along the Paraguay river [4].

Thus, model ages suggest that some distinct "metasomatic events" may have occurred during Paleoproterozoic to Neoproterozoic times as precursor to the alkaline and tholeiitic magmas in the PAE [78].

The significance of model ages is supported by (1) the isotopic overlapping of different igneous rocks (e.g., H-Ti and L-Ti tholeiites or K-alkaline rocks and carbonatites), which cannot be accidental and points to sampling of ancient reservoirs formed at different times from the same subcontinental upper mantle [79]; (2) whatever the implication, that is, heterogeneity induced by recycled crust in the mantle [80, 81], or occurrence of variably veined material in the subcontinental upper mantle, or both [82, 83], Pb isotope data indicate a mantle source of ca. 1.8 Ga for the Paraná H-Ti tholeiites. Since much of the crust in southern Brazil appears to have been formed at ca. 2 Ga ago [84], it follows that magma genesis involved ancient lithospheric mantle reset at well-defined isotopic ranges. A veined lithospheric mantle (amphibole/phlogopite-carbonate-lherzolite and amphibole-lherzolite + CO_2-fluid type III and IV veins of Meen et al. [85] of Proterozoic age) may well account for the magmatism both of the PAE and ASV (Figure 8).

5.3. Mantle Sources. The origin of the ASV magmas is closely related to, and probably constrained by, the geodynamic processes which promoted the generation of the adjacent and coeval magmatism in Brazil [10]. The origin and

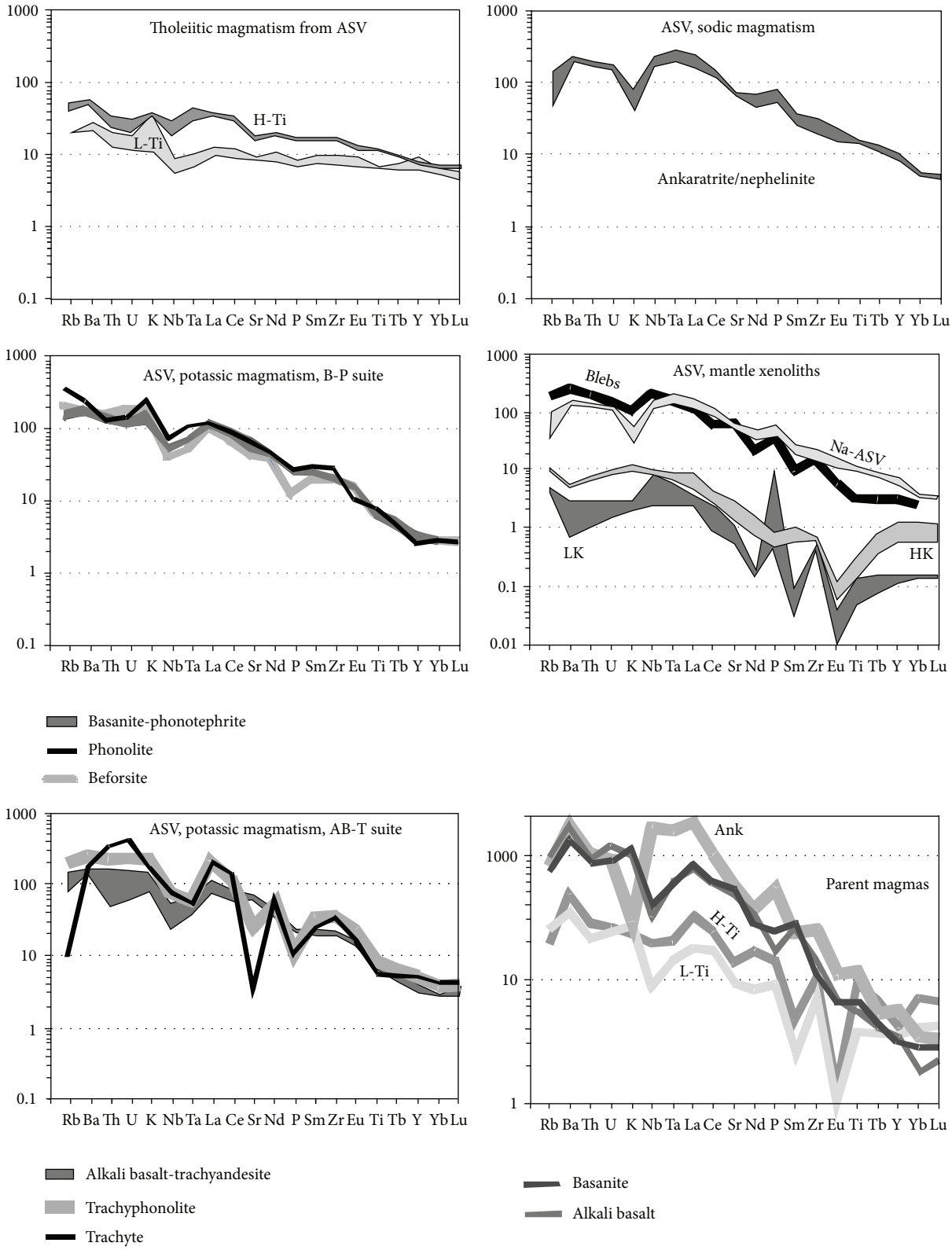

Figure 6: ASV representative compositions (data source as in Tables 1 to 5): incompatible elements normalized to the primitive mantle [86]. Parent magmas: normalizations relative to the calculated parental magmas as proposed by [2, 10, 43, 46]; L-Ti (Mg# 0.64, Ni 250 ppm); H-Ti (Mg# 0.60, Ni 250 ppm); basanite (Mg# 0.74, Ni 710 ppm); alkaline basalt (Mg# 0.74, Ni 323 ppm); ankaratrite (Mg# 0.70, Ni 993 ppm).

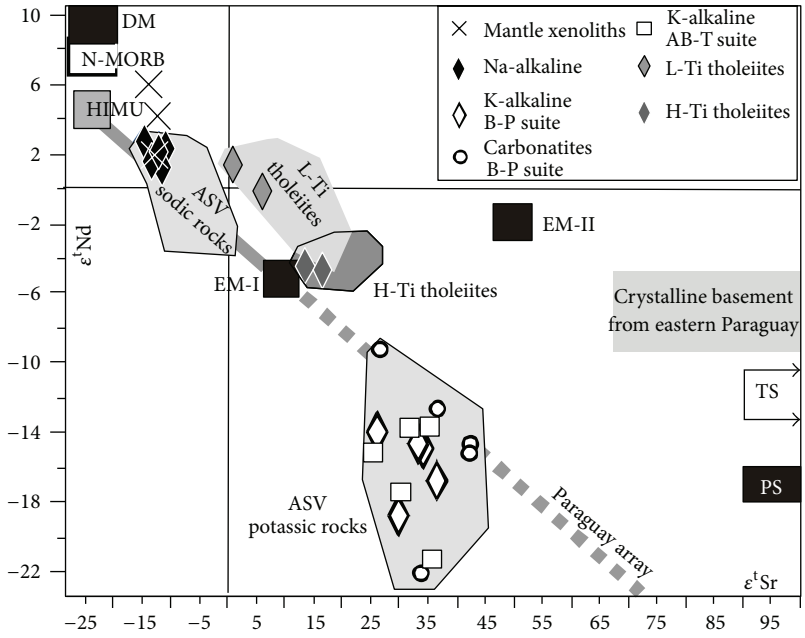

FIGURE 7: Sr and Nd isotopic plot in ε-ε notation: ε_tSr versus ε_tNd correlation diagram for igneous rocks from ASV. Data source: Tables 1 to 5 and [4, 56, 78, 87–89]. DM, HIMU, EMI, and EMII mantle components, terrigenous and pelagic sediments, and TS and PS, respectively [77]; crystalline basement as in [10]. The ε_tSr and ε_tNd time-integrated values were calculated using the following values for Bulk Earth: $^{87}Sr/^{86}Sr = 0.7047$; $^{87}Rb/^{86}Rb = 0.0827$; $^{143}Nd/^{144}Nd = 0.512638$; $^{147}Sm/^{144}Nd = 0.1967$ [50]. Paraguay array is according to [4, 5].

emplacement of the ASV magmatism occurred before, during, and after the opening of the South Atlantic and appears to be related to early stages of lithospheric extension, associated with an anomalously hot mantle [3, 90, 91]. The K/Na and trace element variations and Sr-Nd isotope characteristics of the ASV suites support the view that the lithospheric mantle played an important role in their genesis as well as that of the Paraná flood basalts in Brazil [47, 92, 93].

It should be noted that the most mafic tholeiitic and potassic ASV rock-types are relatively evolved compared with expected primary compositions (e.g., Mg# >0.60–0.65, Ni >235 ppm), ankaratrite is excepted. Possible ASV primary melts (e.g., Mg# ~0.74) in equilibrium with $Fo_{90\text{-}91}$ are expected to have fractionated olivine (Ol) and clinopyroxene (Cpx) at or near the mantle source and certainly during the ascent to the surface [13]. Neglecting the effects of polythermal-polybaric fractionation on the chemistry of the fractionates, crystal fractions have been calculated to restore the selected ASV parental compositions to possible near-primary melts in equilibrium with their mantle sources (cf. Table 3 of [10]).

Mass balance calculations, starting from different garnet-phlogopite peridotites (cf. [94]; whole-rock and mineral compositions in Table 3 of [10] and Table 10 of [43]), indicate that the ASV composition of primary melts can be derived from high and relatively high melting degrees of anhydrous garnet or phlogopite-bearing peridotite, that is, 12 and 30% for tholeiitic basalts (H-Ti and L-Ti, respectively) and 4–11% for the alkaline rock-types (Table 3 of [10]). However, the presence of a relative K enrichment in the ASV potassic and tholeiitic rocks (Figure 6) suggests that a K-bearing phase (e.g., phlogopite) did not represent a residual phase during partial melting. Phlogopite, instead, was probably a residual phase in the mantle source(s) of the ASV sodic rocks. Notably, the parent melts (Figure 6) show high abundances of IE and high LREE/HREE ratios, which require mantle sources enriched in IE before or subcontemporaneously with melting process [94]. Nd model ages approximately indicate that the IE enrichment in the source mantle of the ASV tholeiitic and potassic rocks probably occurred during Paleoproterozoic times (mean 2.03 ± 0.08 Ga), whereas those relative to the sodic rocks would be related to Late Neoproterozoic events (0.57 ± 0.03 Ga). On the other hand, the mantle xenoliths display Nd model ages of 444 ± 11 Ma (cf. Tables 1 to 5).

Concluding, the patterns of the mantle sources of the ASV potassic rocks (along with H-Ti and L-Ti tholeiites) are characterized by negative "Ta-Nb-Ti" and positive Ba and Sm spikes. On the contrary, the patterns of the mantle sources of the ASV sodic rocks (ankaratrites-melanephelinites) show positive Ta-Nb and Zr and negative K and Sm spikes. It seems, therefore, that the genesis of the ASV alkaline magmatism is dominated by a lithospheric mantle, characterized by small-scale heterogeneity, and documented by the occurrence of bleb-like glass in spinel peridotite nodules from the sodic ultramafic rocks [54, 55].

Finally, the isotopic signature of the tholeiitic and K-Na-alkaline-magmatism from the PAE in general, and from ASV in particular, may reflect ancient heterogeneities preserved in the subcontinental lithospheric mantle. As matter of fact, all the geochemical data indicate that the PAE magmatism

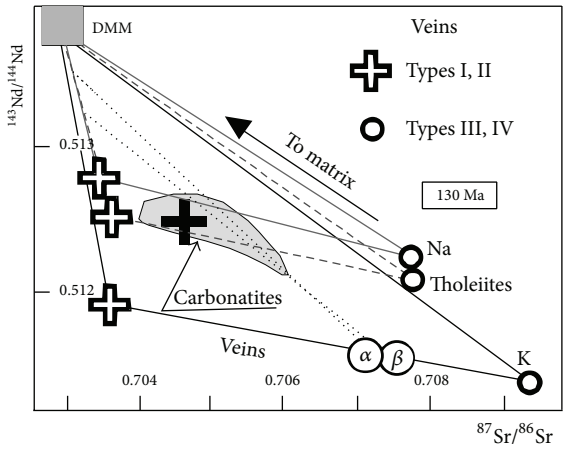

FIGURE 8: Calculated subcontinental upper mantle (SCUM) isotopic composition at 2.0 Ga ago, projected to 130 Ma [85], modified after Figure 10 of [6]. Parental melts with various Rb/Sr and Sm/Nd ratios are assumed for K, Na (potassic and sodic rocks from ASV [10]), and PAE tholeiites [3]. It should be noted that the compositions of metasomites formed from a single metasomatizing melt vary with the evolution of the melt. Consequently, the veins will define a trend of shallow slope, and mixing curves between vein and matrix will define an array towards the matrix (cf. α and β regression lines). Model depleted mantle (DMM): Rb = 0, Sr = 0.133, Sm = 0.314, and Nd = 0.628; present day Bulk Earth: $^{87}Sr/^{86}Sr$ = 0.70475, $^{87}Rb/^{86}Sr$ = 0.0816, $^{143}Nd/^{144}Nd$ = 0.512638, and $^{147}Sm/^{143}Nd$ = 0.1967; $(Rb/Sr)_{diopside} : (Rb/Sr)_{melt} \approx 0.125$, $(Sm/Nd)_{diopside} : (Sm/Nd)_{melt} \approx 1.5$; K : Rb/Sr = 0.0957, Sm/Nd = 0.1344; Na : Rb/Sr = 0.0732, Sm/Nd = 0.2295; Th : Rb/Sr = 0.0733, Sm/Nd = 0.2082.

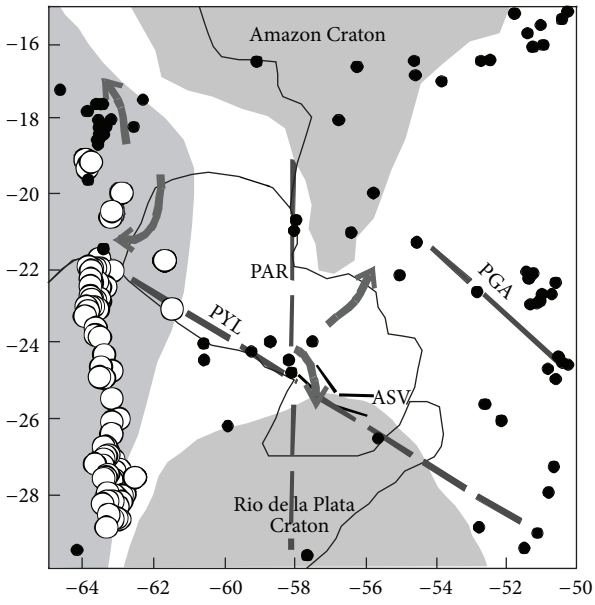

FIGURE 9: Earthquakes distribution at the Paraguay and neighbouring regions: open and full circles, earthquake hypocenters >500 and <70 km, respectively [29]. Heavy black lines indicate extensional lineaments: PGA, Ponta Grossa Arch; PAR and PYL, Paraguays and Pylcomaio lineaments, respectively (cf. also inset of Figure 3). The dark grey delineates the rotational subplate trends [24, 95]. ASV: Asunción-Sapucai-Villarrica graben.

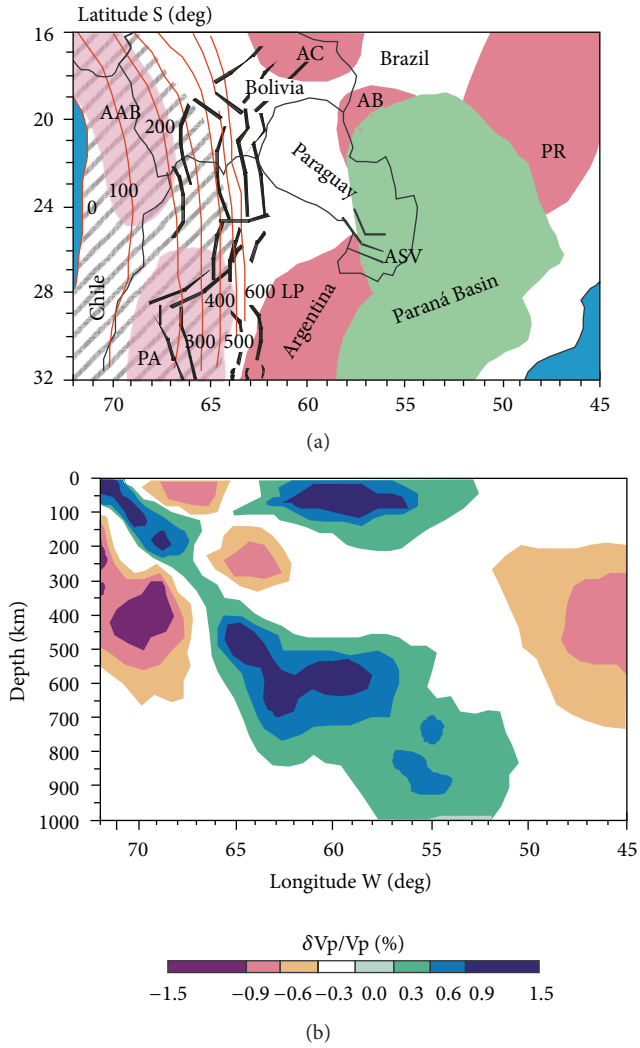

FIGURE 10: (a) General map, including ASV, showing contours (red lines) of the depth (km) of the subducting Nazca slab based on seismic data of [96]. Heavy lines (black) outline the Cretaceous rift systems. The hatched area roughly marks the extension of intense early Paleozoic reworking of Proterozoic material, but the exact border to the Brazilian Craton remains unknown [97]. Pink fields delineate inferred positions of major cratonic fragments below Phanerozoic cover [98]: AAB, Arequipa-Antofalla; AC, Amazon Craton; AB, Apa Block; PR, Paranapanema; LP, Rio de la Plata; PA, Pampia. (b) Seismic tomography image [99] across a profile approximately at 24° Lat. S. Note that the low-velocity feature in the mantle to the East has been interpreted as a fossil mantle plume [100].

requires heterogeneous mantle sources, also in terms of radiogenic isotopes [6, 10]: such heterogeneities probably represent metasomatic processes which have occurred mainly at 0.5–1.0 Ga and at 1.5–2.0 Ga (cf. T_{DM} of Tables 1–4).

6. Geodynamic Implications

Some general considerations on the geodynamics are discussed in [4–6, 87–89]. The ASV geodynamic evolution is

related to that of the Western Gondwana (Figure 1), which reflects the regional amalgamation processes and requires an overall understanding of the pre-Gondwanic setting, at least at the time of the Brasiliano cycle, both at the Atlantic and Pacific systems. The Brasiliano cycle was developed diachronically between about 890 and 480 Ma, until the final basement of the South American Platform was attained [101]. This occurred during the Lower Ordovician, where Unrug [102] suggested a mosaic of lithospheric fragments linked by several (accretionary, collisional) Neoproterozoic mobile belts. After amalgamation, the Gondwana supercontinent accumulated Paleozoic and Triassic-Jurassic sediments. Concomitantly, it was continuously and laterally accreted to the western borders by successive orogenic belts, until the Pangea Formation [103, 104]. The main cratonic fragments descending from ancestors of the Pangea, for example, the Amazonic and Rio de La Plata cratons, were revoked, and smaller ancient crustal blocks formed at the Paraguay boundaries [105]. The magmatism was likely driven by the relative extensional regimes derived from the relative movements of the ancient blocks (Figure 9), probably induced by counterclockwise and clockwise movements (North and South, resp.) hinged at about 20° and 24°S [106].

The earthquake distribution and mechanisms [29] with hypocenters >500 km and <70 km, respectively (Figure 9), coincide with the inferred Nazca plate subduction at the Paraguay latitude (Figure 10), where the depth of the lithospheric earthquakes, together with the paleomagnetic results [38, 95, 107], delineates different rotational paths at about 18–24°S (i.e., Chaco-Pantanal Basin). These data indicate extensional subplate tectonics along the Andean system [95], coupled with the lineaments of lithospheric earthquakes versus the Atlantic system that parallels the Ponta Grossa Arch and the lineaments of Rio Paraguay and Rio Pilcomayo, also clearly related to extensional environments [24, 29, 78].

Crucial to the genesis of the ASV magma types is the link with the whole PAE system and with the geodynamic processes responsible for the opening of the South Atlantic. According to Nürberg and Müller [108], the sea-floor spreading in the South Atlantic at ASV latitude started at about 125–127 Ma (Chron M4), but North of the Walvis-Rio Grande ridge (Figure 1(b)) the onset of the oceanic crust would be younger, for example, 113 Ma [109]. Therefore, the Early Cretaceous alkaline and alkaline-carbonatite complexes from ASV (and PAE) are subcoeval with respect to the main flood tholeiites of the Paraná Basin and occurred during the early stages of rifting, before the main continental separation.

The origin of alkaline-carbonatitic magmatism in terms of plate tectonics is currently debated [77, 110] and often considered in terms of models only. In the present context, the different westward angular velocity of the lithospheric fragments in the South American plate, as defined by the "second order plate boundaries" (e.g., the Pylcomaio lineament [18]) as well as the different rotational trends at S19–24° Latitude, would favour decompression and melting at different times of variously metasomatized (wet spot) portion of the lithospheric mantle with variable isotopic signatures [24]. Small-scale metasomatism is indicated by the different suites of mantle xenoliths and significant H-O-C and F variations, expected in the mantle source from the occurrence of the related carbonatites. The latter imply lowering of the solidus and, along with an extensional tectonic, favour the melting of the mantle and magma ascent. This scenario also accounts for the presence of Late Cretaceous to Tertiary sodic magmatism in the PAE and in the Eastern Paraguay, where rifting structures are evident (cf. Figures 2 and 4).

7. Concluding Remarks

Geological and geophysical results show that the Mesozoic-Tertiary block-faulting tectonics in Eastern Paraguay is responsible for NW-trending grabens (ASV and Amambay), fault systems, and fault-controlled basins, for example, Jejui-Aguaray-Guazu, Asunción-Encarnación, San Pedro (cf. Figure 2).

Distinct magmatic events are widespread in the Asunción-Sapucai-Villarrica graben, the major extensional structure in Eastern Paraguay, that is, Early Cretaceous tholeiites and K-alkaline-carbonatitic complexes and dykes, along with Tertiary sodic magmatism. It is expected that beneath a rifted continental area, as ASV, the lithospheric mantle may have been thinned and subjected to high heat flow. This allowed the geotherm to intersect the peridotite solidus in the presence of H_2O-CO_2-rich fluids and favour the melt formations. Under these conditions, the derived melts may form, dissolving most of the "volatile" phases and, percolating through a porous and deformed rock matrix, invaded the base of the lithosphere and favoured metasomatic processes at different levels in the peridotitic lithosphere with the formation of amphibole and/or phlogopite ("veined mantle" of [82, 83]). Notably, the different tholeiitic (high- and low-Ti), K-alkaline suites (B-P and Ab-T), and sodic magmatism with HK and LK xenoliths are consistent with variously depleted lithospheric mantle at different times, pervasively and locally invaded by metasomatizing fluids and/or melts. Thereafter, the newly formed veins ("enriched component") and peridotitic matrix ("depleted component") undervent different isotopic compositions with time, depending on their parent/daughter ratio (cf. Figure 8), testifying heterogeneous mantle sources beneath ASV.

Acknowledgments

This paper is dedicated to the memory of Enzo Michele Piccirillo who was an inspiration to the authors over many years of geological work in the region. P. Comin-Chiaramonti gratefully acknowledges CNR and MURST (Italian Agencies) for the field financial support since 1981 and the Department of Geosciences of the Trieste University for the use of chemical laboratories where all the analyses were performed. Thanks are due to Exxon Co., USDMA, ITAIPU, and YACIRETA (Paraguayan Agencies) for their collaborations and to engineer E. Debernardi (deceased) and geologists D. Orué, Luis Lúcia, and L. A. Martinez. This research was also supported by grants (Procs. 08/3807-4 and 10/50887-3) to C. B. Gomes from the Brazilian agency Fapesp.

The Ms benefit of the accurate revision of Keith Bell and Lalou Gwalani.

References

[1] V. C. Velázquez, C. B. Gomes, C. Riccomini, and J. Kirk, "The cretaceous alkaline dyke swarm in the central segment of the Asunción rift, eastern Paraguay: its regional distribution, mechanism of emplacement, and tectonic significance," *Journal of Geological Research*, vol. 2011, Article ID 946701, 18 pages, 2011.

[2] G. Bellieni, P. C. Chiaramonti, L. S. Marques et al., "Continental flood basalts from the central-western regions of the Parana plateau (Paraguay and Argentina): petrology and petrogenetic aspects," *Neues Jahrbuch für Mineralogie, Abhandlungen*, vol. 154, no. 2, pp. 111–139, 1986.

[3] E. M. Piccirillo and A. J. Melfi, Eds., *The Mesozoic Flood Volcanism of the Paranà Basin: Petrogenetic and Geophysical Aspects*, IAG, São Paulo, Brazil, 1988.

[4] P. Comin-Chiaramonti, A. Marzoli, C. De Barros Gomes et al., "The origin of post-Paleozoic magmatism in eastern Paraguay," *Special Paper of the Geological Society of America*, no. 430, pp. 603–633, 2007.

[5] P. Comin-Chiaramonti, C. B. Gomes, M. Ernesto, A. Marzoli, and C. Riccomini, *Eastern Paraguay: Post-Paleozoic Magmatism*, Large Igneous Province of the Month, 2007, http://www.largeigneousprovinces.org/07jan .

[6] P. Comin-Chiaramonti, A. De Min, V. A. V. Girardi, and E. Ruberti, "Post-Paleozoic magmatism in Angola and Namibia: a review," in *Volcanism and Evolution of the African Lithosphere, the Geological Society of America*, L. Beccaluva, G. Bianchini, and M. Wilson M, Eds., Special Paper 478, pp. 223–247, 2011.

[7] J. D. Fairhead and M. Wilson, "Plate tectonic processes in the South Atlantic Ocean: do we need deep mantle plumes?" *Special Paper of the Geological Society of America*, no. 388, pp. 537–553, 2005.

[8] P. V. Zalan, S. Wolff, M. A. Astolfi et al., "The Paraná basin, Brazil," in *Interior Cratonic Basins*, M. W. Leighton, D. R. Kolata, D. F. Oltz, and J. J. Eidel, Eds., vol. 51 of *Memoir*, pp. 601–708, American Association of Petroleum Geology, Tulsa, Okla, USA, 1990.

[9] J. J. W. Rogers, R. Unrug, and M. Sultan, "Tectonic assembly of Gondwana," *Journal of Geodynamics*, vol. 19, no. 1, pp. 1–34, 1995.

[10] P. Comin-Chiaramonti, A. Cundari, E. M. Piccirillo et al., "Potassic and sodic igneous rocks from Eastern Paraguay: their origin from the lithospheric mantle and genetic relationships with the associated Paraná flood tholeiites," *Journal of Petrology*, vol. 38, no. 4, pp. 495–528, 1997.

[11] M. Feng, V. D. S. Lee, and M. Assumpção, "Upper mantle srructure of South America from joint inversions of waveforms and fundamental mode group velocities of Rayleigh waves," *Journal of Geophysical Research*, vol. 112, pp. 1–16, 2007.

[12] P. Comin-Chiaramonti, A. Cundari, J. M. DeGraff, C. B. Gomes, and E. M. Piccirillo, "Early Cretaceous-Tertiary magmatism in Eastern Paraguay (western Parana basin): geological, geophysical and geochemical relationships," *Journal of Geodynamics*, vol. 28, no. 4-5, pp. 375–391, 1999.

[13] P. Comin-Chiaramonti, A. Cundari, C. B. Gomes et al., "Potassic dyke swarm in the Sapucai Graben, eastern Paraguay: petrographical, mineralogical and geochemical outlines," *LITHOS*, vol. 28, no. 3–6, pp. 283–301, 1992.

[14] C. Riccomini, V. F. Velázquez, and C. De Barros Gomes, "Cenozoic lithospheric faulting in the Asunción Rift, eastern Paraguay," *Journal of South American Earth Sciences*, vol. 14, no. 6, pp. 625–630, 2001.

[15] Anschutz Co., *Geologic Map of Eastern Paraguay (1:500,000)*, F. Wiens Compiler, Denver, Colo, USA, 1981.

[16] M. D. Druecker and S. P. Gay Jr., "Mafic dyke swarms associated with Mesozoic rifting in Eastern Paraguay, South America," in *Mafic Dyke Swarms, Geological Association of Canada*, H. C. Halls and A. R. Fahrig, Eds., pp. 187–193, 1987.

[17] N. Ussami, A. Kolisnyk, M. I. B. Raposo, F. J. F. Ferreira, E. C. Molina, and M. Ernesto, "Detectabilitade magnetica de diques do Arco de Ponta Grossa: um estudo integrado de magnetometria terrestre/aerea e magnetismo de rocha," *Revista Brasileira de Geociências*, vol. 21, pp. 317–327, 1994.

[18] J. M. de Graff, "Late Mesozoic crustal extension and rifting on the western edge of the Paraná Basin, Paraguay," *Geological Society of America, Abstracts with Programs*, vol. 17, p. 560, 1985.

[19] PHOTO GRAVITY Co., *Regional Bouguer Gravity Data and Station Location Map of the Paraguay (Scale 1:2,000,000)*, Archivo DRM-MOPC, Asunción, Paraguay, 1991.

[20] D. S. Hutchinson, "Geology of the Apa High," Internal Report, TAC, Asunción, Paraguay, 1979.

[21] F. Wiens, "Mapa geologica de la region oriental, Republica del Paraguay, escala 1:500,0002," *Simposio Recursos Naturales, Paraguay, Asunción*, p. 9, 1982.

[22] R. A. Livieres and H. Quade, "Distribución regional y asentamiento tectónico de los complejos alcalinos del Paraguay," *Zentralblatt für Geologie und Paläontologie*, vol. 7, pp. 791–805, 1987.

[23] A. Kanzler, "The southern Precambrian in Paraguay. Geological inventory and age relations," *Zentralblatt für Geologie und Paläontologie*, vol. 7, pp. 753–765, 1987.

[24] P. Comin-Chiaramonti and C. B. Gomes, Eds., *Alkaline Magmatism in Central-Eastern Paraguay. Relationships with Coeval Magmatism in Brazil*, Edusp/Fapesp, São Paulo, Brazil, 1996.

[25] P. R. Renne, M. Ernesto, I. G. Pacca et al., "The age of Paraná flood volcanism, rifting of gondwanaland, and the Jurassic-Cretaceous boundary," *Science*, vol. 258, no. 5084, pp. 975–979, 1992.

[26] P. R. Renne, D. F. Mertz, W. Teixeira, H. Ens, and M. Richards, "Geochronologic constraints on magmatic and tectonic evolution of the Paraná Province," *The American Geophysical Union*, vol. 74, abstract, p. 553, 1993.

[27] P. R. Renne, K. Deckart, M. Ernesto, G. Féraud, and E. M. Piccirillo, "Age of the Ponta Grossa dike swarm (Brazil), and implications to Paraná flood volcanism," *Earth and Planetary Science Letters*, vol. 144, no. 1-2, pp. 199–211, 1996.

[28] C. B. Gomes, P. Comin-Chiaramonti, and V. F. Velázquez, "The Mesoproterozoic rhyolite occurrences of Fuerte Olimpo and Fuerte San Carlos, Northern Paraguay," *Revista Brasileira De Geociências*, vol. 30, pp. 785–788, 2000.

[29] J. Berrocal and C. Fernandes, "Seismicity in Paraguay and neighbouring regions," in *Alkaline Magmatism in Central-Eastern Paraguay, Relationships with Coevalmagmatism in Brazil*, P. Comin-Chiaramonti and C. B. Gomes, Eds., pp. 57–66, Edusp/Fapesp, São Paulo, Brazil, 1996.

[30] A. Tommasi and A. Vauchez, "Continental rifting parallel to ancient collisional belts: an effect of the mechanical anisotropy of the lithospheric mantle," *Earth and Planetary Science Letters*, vol. 185, no. 1-2, pp. 199–210, 2001.

[31] P. F. Green, I. R. Duddy, P. O'Sullivan, K. A. Hegarty, P. Comin-Chiaramonti, and C. B. Gomes, "Mesozoic potassic magmatism from the Asunción-Sapucai graben: apatite fission track analysis of the Acahai suite and implication for hydrocarbon exploration," *Geochimica Brasiliensis*, vol. 5, pp. 79–88, 1991.

[32] K. A. Hegarty, I. R. Duddy, and P. F. Green, "The thermal history in around the Paraná basin using apatite fission track analysis-implications for hydrocarbon occurrences and basin formation," in *Alkaline magmatism in Central-Eastern Paraguay, Relationships with Coevalmagmatism in Brazil*, P. Comin-Chiaramonti and C. B. Gomes, Eds., pp. 67–84, Edusp/Fapesp, São Paulo, Brazil, 1996.

[33] P. Comin-Chiaramonti, A. De Min, and C. B. Gomes, "Magmatic rock-types from the Asunción-Sapucai graben: description of the occurrences and petrographical notes," in *Alkaline Magmatism in Central-Eastern Paraguay, Relationships with coevalmagmatism in Brazil*, P. Comin-Chiaramonti and C. B. Gomes, Eds., pp. 275–330, Edusp/Fapesp, São Paulo, Brazil, 1996.

[34] P. Comin-Chiaramonti, A. De Min, and A. Marzoli, "Magmatic rock-types from the Asunción-Sapucai graben: chemical analyses," in *Alkaline Magmatism in Central-Eastern Paraguay, Relationships with coevalmagmatism in Brazil*, P. Comin-Chiaramonti and C. B. Gomes, Eds., pp. 331–387, Edusp/Fapesp, São Paulo, Brazil, 1996.

[35] P. Comin-Chiaramonti, A. Cundari, and G. Bellieni, "Mineral analyses of alkaline rock-types from the Asunción-Sapucai graben," in *AlkalIne Magmatism in Central-Eastern Paraguay, Relationships with coevalmagmatism In Brazil*, P. Comin-Chiaramonti and C. B. Gomes, Eds., pp. 389–458, Edusp/Fapesp, São Paulo, Brazil, 1996.

[36] P. Comin-Chiaramonti, A. Cundari, A. De Min, C. B. Gomes, and V. F. Velázquez, "Magmatism in Eastern Paraguay: occurrence and petrography," in *Alkaline Magmatism in Central-Eastern Paraguay, Relationships with coevalmagmatism in Brazil*, P. Comin-Chiaramonti and C. B. Gomes, Eds., pp. 103–122, Edusp/Fapesp, São Paulo, Brazil, 1996.

[37] J. M. de Graff, S. P. Gay Jr., and D. Orué, "Interpretación geofísica and geológica del Valle de Ypacaraí (Paraguay) y su formación," *Revista de la Asociación Geológica Argentina*, vol. 36, no. 3, pp. 240–256, 1981.

[38] M. Ernesto, P. Comin-Chiaramonti, C. B. Gomes, A. M. C. Castillo, and V. F. Velazquez, "Palaeomagnetic data from the central alkaline province, Eastern Paraguay," in *Alkaline Magmatism in Central-Eastern Paraguay, Relationships with coevalmagmatism in Brazil*, P. Comin-Chiaramonti and C. B. Gomes, Eds., pp. 85–102, Edusp/Fapesp, São Paulo, Brazil, 1996.

[39] H. de La Roche, "Classification and nomenclature des roches ignées: un essai de restauration de la convergence entre systématique quantitative, typologie d'usage et modélisation génétique," *Bulletin de la Societé Geologique de France*, vol. 8, pp. 337–353, 1986.

[40] R. P. Le Maitre, *A Classification of Igneous Rocks and Glossary of Terms*, Blackwell, Oxford, UK, 1989.

[41] A. Streckeisen, "To each plutonic rock its proper name," *Earth Science Reviews*, vol. 12, no. 1, pp. 1–33, 1976.

[42] C. B. Gomes, P. Comin-Chiaramonti, A. DeMin et al., "Atividade filoniana asociada ao complexo alcalino de Sapukai, Paraguay Oriental," *Geochimica Brasiliensis*, vol. 3, pp. 93–114, 1989.

[43] G. Bellieni, P. Comin-Chiaramonti, L. S. Marques et al., "Petrogenetic aspects of acid and basaltic lavas from the Paraná plateau (Brazil): geological, mineralogical and petrochemical relationships," *Journal of Petrology*, vol. 27, no. 4, pp. 915–944, 1986.

[44] P. Comin-Chiaramonti, C. B. Gomes, P. Censi, A. DeMin, S. Rotolo, and V. F. Velazquez, "Geoquimica do magmatismo Post-Paleozoico no Paraguai Centro-Oriental," *Geochimica Brasiliensis*, vol. 7, pp. 19–34, 1993.

[45] G. Bellieni, P. Comin-Chiaramonti, L. S. Marques et al., "High- and low-TiO_2 flood basalts of Paraná plateau (Brazil): petrology, petrogenetic aspects and mantle source relationships," *Neues Jahrbuch für Mineralogie Abhandlungen*, vol. 150, pp. 273–306, 1984.

[46] E. M. Piccirillo, G. Bellieni, P. Comin-Chiaramonti et al., "Continental flood volcanism from the Parana' Basin (Brazil)," in *Continental Flood Volcanism*, J. D. McDougal, Ed., pp. 195–238, Kluver Academic, London, UK, 1988.

[47] E. M. Piccirillo, L. Civetta, R. Petrini et al., "Regional variations within the Paraná flood basalts (southern Brazil): evidence for subcontinental mantle heterogeneity and crustal contamination," *Chemical Geology*, vol. 75, no. 1-2, pp. 103–122, 1989.

[48] P. Comin-Chiaramonti, P. Censi, A. Cundari, and C. B. Gomes, "A silico-beforsitic flow from the Sapucai Complex (central-eastern Paraguay)," *Geochimica Brasiliensis*, vol. 6, no. 1, pp. 87–91, 1992.

[49] P. Comin-Chiaramonti, A. Cundari, C. B. Gomes et al., "Mineral chemistry and its genetic significance of major and accessory minerals from a potassic dyke swarm in the Sapucai graben, Central-Eastern Paraguay," *Brasileira Geoquímica*, vol. 4, pp. 175–206, 1990.

[50] G. Faure, *Origin of Igneous Rocks: The Isotopic Evidence*, Springer, Berlin, Germany, 2001.

[51] A. D. Edgar, "Role of subduction in the genesis of leucite-bearing rocks: discussion," *Contributions to Mineralogy and Petrology*, vol. 73, no. 4, pp. 429–431, 1980.

[52] A. Cundari and A. K. Ferguson, "Significance of the pyroxene chemistry from leucite-bearing and related assemblages," *TMPM Tschermaks Mineralogische und Petrographische Mitteilungen*, vol. 30, no. 3, pp. 189–204, 1982.

[53] P. Comin-Chiaramonti, F. Lucassen, V. A. V. Girardi, A. De Min, and C. B. Gomes, "Lavas and their mantle xenoliths from intracratonic eastern Paraguay (South America Platform) and andean domain, NW-Argentina: a comparative review," *Mineralogy and Petrology*, vol. 98, no. 1-2, pp. 143–165, 2010.

[54] G. DeMarchi, P. Comin-Chiaramonti, P. DeVito, S. Sinigoi, and A. M. C. Castillo, "Lherzolite-dunite xenoliths from Eastern Paraguay: petrological constraints to mantle metasomatism," in *The Mesozoic Flood Volcanism of the Paran' Basin: Petrogenetic and Geophysical Aspects*, E. M. Piccirillo and A. J. Melfi, Eds., pp. 207–228, IAG, São Paulo, Brazil, 1988.

[55] P. Comin-Chiaramonti, L. Civetta, E. M. Piccirillo et al., "Tertiary nephelinitic magmatism in eastern Paraguay: petrology, Sr- Nd isotopes and genetic relationships with associated spinel-peridotite xenoliths," *European Journal of Mineralogy*, vol. 3, no. 3, pp. 507–525, 1991.

[56] P. Comin-Chiaramonti, F. Princivalle, V. A. V. Girardi, C. B. Gomes, A. Laurora, and R. Zanetti, "Mantle xenoliths from Ñemby, Eastern Paraguay: O-Sr-Nd isotopes, trace elements and crystal chemistry of hosted clinopyroxenes," *Periodico di Mineralogia*, vol. 70, pp. 205–230, 2001.

[57] J. Wang, K. H. Hattori, R. Kilian, and C. R. Stern, "Metasomatism of sub-arc mantle peridotites below southernmost

South America: reduction of fO_2 by slab-melt," *Contributions to Mineralogy and Petrology*, vol. 153, no. 5, pp. 607–624, 2007.

[58] M. F. Roden, F. A. Frey, and D. M. Francis, "An example of consequent mantle metasomatism in peridotite inclusions from Nunivak Island, Alaska," *Journal of Petrology*, vol. 25, no. 2, pp. 546–577, 1984.

[59] S. Y. O'Reilly and W. L. Griffin, "Mantle metasomatism beneath western Victoria, Australia: I. Metasomatic processes in Cr-diopside lherzolites," *Geochimica et Cosmochimica Acta*, vol. 52, no. 2, pp. 433–447, 1988.

[60] F. J. Spera, "Carbon dioxide in petrogenesis III: role of volatiles in the ascent of alkaline magma with special reference to xenolith-bearing mafic lavas," *Contributions to Mineralogy and Petrology*, vol. 88, no. 3, pp. 217–232, 1984.

[61] F. A. Frey and D. H. Green, "The mineralogy, geochemistry and origin of lherzolite inclusions in Victorian basanite," *Geochimica et Cosmochimica Acta*, vol. 38, pp. 1023–1050, 1979.

[62] D. K. Koustpoulos, "Melting of the shallow upper mantle: a new perspective," *Journal of Perology*, vol. 32, pp. 671–699, 1991.

[63] G. Rivalenti, R. Vannucci, E. Rampone et al., "Peridotite clinopyroxene chemistry reflects mantle processes rather than continental versus oceanic settings," *Earth and Planetary Science Letters*, vol. 139, no. 3-4, pp. 423–437, 1996.

[64] P. R. A. Wells, "Pyroxene thermometry in simple and complex systems," *Contributions to Mineralogy and Petrology*, vol. 42, pp. 109–121, 1977.

[65] J. Fabriès, "Spinel-olivine geothermometry in peridotites from ultramafic complexes," *Contributions to Mineralogy and Petrology*, vol. 69, pp. 329–336, 1979.

[66] J. C. Mercier, "Single-pyroxene geothermometry and geobarometry," *The American Journal of Sciences*, vol. 61, no. 7-8, pp. 603–615, 1980.

[67] J. C. C. Mercier, V. Benoit, and J. Girardeau, "Equilibrium state of diopside-bearing harzburgites from ophiolites: geobarometric and geodynamic implications," *Contributions to Mineralogy and Petrology*, vol. 85, no. 4, pp. 391–403, 1984.

[68] G. Sen, F. A. Frey, N. Shimizu, and W. P. Leeman, "Evolution of the lithosphere beneath Oahu, Hawaii: rare earth element abundances in mantle xenoliths," *Earth and Planetary Science Letters*, vol. 119, no. 1-2, pp. 53–69, 1993.

[69] H. Chiba, T. Chack, R. N. Clayton, and J. Goldsmith, "Oxygen isotope fractionations involving diopside, forsterite, magnetite, and calcite: application to geothermometry," *Geochimica et Cosmochimica Acta*, vol. 53, pp. 2985–2989, 1989.

[70] D. Mattey, D. Lowry, and C. Macpherson, "Oxygen isotope composition of mantle peridotite," *Earth and Planetary Science Letters*, vol. 128, no. 3-4, pp. 231–241, 1994.

[71] T. K. Kyser, "1990. Stable isotopes in the continental lithospheric mantle," in *Continental Mantle*, M. A. Menzies, Ed., pp. 127–156, Oxford Clarendon Press, Oxford, UK, 1990.

[72] T. K. Kyser, J. R. O'Neil, and I. S. E. Carmichael, "Oxygen isotope thermometry of basic lavas and mantle nodules," *Contributions to Mineralogy and Petrology*, vol. 77, no. 1, pp. 11–23, 1981.

[73] F. Princivalle, M. Tirone, and P. Comin-Chiaramonti, "Clinopyroxenes from metasomatized spinel-peridotite mantle xenoliths from Nemby (Paraguay): crystal chemistry and petrological implications," *Mineralogy and Petrology*, vol. 70, no. 1-2, pp. 25–35, 2000.

[74] F. Castorina, P. Censi, P. Comin-Chiaramonti et al., "Carbonatites from Eastern Paraguay and genetic relationships with potassic magmatism: C, O, Sr and Nd isotopes," *Mineralogy and Petrology*, vol. 61, no. 1–4, pp. 237–260, 1998.

[75] P. Antonini, M. Gasparon, P. Comin-Chiaramonti, and C. B. Gomes, "Post-palaeozoic magmatism in Eastern paraguay: Sr-Nd-Pb isotope compositions," in *Mesozoic to Cenozoic Alkaline Magmatism in the Brazilian Platform*, P. Comin-Chiaramonti and C. B. Gomes, Eds., pp. 57–70, EdUSP, Fapesp, São Paulo, Brazil, 2005.

[76] D. Mckenzie and R. K. O'nions, "The source regions of ocean island basalts," *Journal of Petrology*, vol. 36, no. 1, pp. 133–159, 1995.

[77] S. R. Hart and A. Zindler, "Constraints on the nature and the development of chemical heterogeneities in the mantle," in *Mantle Convection Plate Tectonics and Global Dynamics*, W. R. Peltier, Ed., pp. 261–388, Gordon and Breach Sciences, New York, NY, USA, 1989.

[78] P. Comin-Chiaramonti, C. B. Gomes, and Eds, *Mesozoic to Cenozoic Alkaline Magmatism in the Brazilian Platform*, EdUSP, Fapesp, São Paulo, Brazil, 2005.

[79] R. W. Carlson, S. Esperança, and D. P. Svisero, "Chemical and Os isotopic study of Cretaceous potassic rocks from Southern Brazil," *Contributions to Mineralogy and Petrology*, vol. 125, no. 4, pp. 393–405, 1996.

[80] M. A. Menzies, Ed., *Continental Mantle*, Oxford Clarendon Press, 1990.

[81] B. L. Weaver, "The origin of ocean island basalt end-member compositions: trace element and isotopic constraints," *Earth and Planetary Science Letters*, vol. 104, no. 2–4, pp. 381–397, 1991.

[82] S. Foley, "Petrological characterization of the source components of potassic magmas: geochemical and experimental constraints," *LITHOS*, vol. 28, no. 3–6, pp. 187–204, 1992.

[83] S. Foley, "Vein-plus-wall-rock melting mechanisms in the lithosphere and the origin of potassic alkaline magmas," *LITHOS*, vol. 28, no. 3–6, pp. 435–453, 1992.

[84] C. J. Hawkesworth, M. S. M. Mantovani, P. N. Taylor, and Z. Palacz, "Evidence from the Parana of south Brazil for a continental contribution to Dupal basalts," *Nature*, vol. 322, no. 6077, pp. 356–359, 1986.

[85] J. K. Meen, J. C. Ayers, and E. J. Fregeau, "A model of mantle metasomatism by carbonated alkaline melts: trace element and isotopic compositions of mantle source regions of carbonatite and other continental igneous roks," in *Carbonatites, Genesis and Evolution*, K. Bell, Ed., pp. 464–499, Unwin Hyman, London, UK, 1989.

[86] S.-S. Sun and W. F. McDonough, "Chemical and isotopic systematics of oceanic basalts: implications for mantle composition and processes," in *Magmatism in the Ocean Basins*, A. D. Saunders and M. J. Norry, Eds., Special Paper 42, pp. 313–345, Geological Society of London, 1989.

[87] P. Comin-Chiaramonti, F. Castorina, A. Cundari, R. Petrini, and C. B. Gomes, "Dykes and sills from Eastern paraguay: Sr and Nd isotope systematic," in *IDC-3, Physics and Chemistry of Dykes*, G. Baer and A. Heiman, Eds., pp. 267–278, Balkema, Rotterdam, The Netherlands, 1995.

[88] P. Comin-Chiaramonti, C. B. Gomes, A. Cundari, F. Castorina, and P. Censi, "A review of carbonatitic magmatism in the Paraná-Angola-Etendeka (Pan) system," *Periodico di Mineralogia*, vol. 76, pp. 25–78, 2007.

[89] P. Comin-Chiaramonti, C. B. Gomes, P. Censi et al., "Alkaline complexes from the alto paraguay province at the border of Brazil (Mato Grosso do Sul State) and Paraguay," in *Mesozoic To Cenozoic Alkaline Magmatism in the Brazilian Platform*, P. Comin-Chiaramonti and C. B. Gomes, Eds., pp. 71–148, Eduspp-Fapesp, SãoPaulo, Brazil, 2005.

[90] C. J. Hawkesworth, K. Gallagher, S. Kelley et al., "Paraná magmatism and the opening of the South Atlantic," in *Magmatism and the Causes of Continental Break-Up*, B. C. Storey, Ed., vol. 68, pp. 221–240, Geological Society of London, 1992.

[91] S. Turner, M. Regelous, S. Kelley, C. Hawkesworth, and M. Mantovani, "Magmatism and continental break-up in the South Atlantic: high precision $^{40}Ar^{39}Ar$ geochronology," *Earth and Planetary Science Letters*, vol. 121, no. 3-4, pp. 333–348, 1994.

[92] D. W. Peate, "The parana-etendeka province," in *Large Igneuos Province: Continetal Oceanic, Planetary Flood Volcanism*, J. Mahoney and M. F. Coffin, Eds., pp. 217–245, American Geophyscial Union, Washington, DC, USA, 1992.

[93] D. W. Peate and C. J. Hawkesworth, "Lithospheric to asthenospheric transition in low-Ti flood basalts from southern Paraná, Brazil," *Chemical Geology*, vol. 127, no. 1–3, pp. 1–24, 1996.

[94] A. J. Erlank, F. G. Waters, C. J. Hawkesworth et al., "Evidence for mantle metasomatism in peridotite nodules from the Kimberley pipes, South Africa," in *Mantle Metasomatism*, M. A. Menzies and C. J. Hawkesworth, Eds., pp. 221–309, Academic Press, London, UK, 1987.

[95] D. E. Randall, "A new Jurassic-Recent apparent polar wander path for South America and a review of central Andean tectonic models," *Tectonophysics*, vol. 299, no. 1–3, pp. 49–74, 1998.

[96] O. Gudmundsson and M. Sambridge, "A Regionalized Upper Mantle (RUM) seismic model," *Journal of Geophysical Research B*, vol. 103, no. 4, pp. 7121–7136, 1998.

[97] F. Lucassen, R. Becchio, H. G. Wilke et al., "Proterozoic-Paleozoic development of the basement of the Central Andes (18-26°S) - A mobile belt of the South American craton," *Journal of South American Earth Sciences*, vol. 13, no. 8, pp. 697–715, 2000.

[98] J. H. Laux, M. M. Pimentel, E. L. Dantas, R. Armstrong, and S. L. Junges, "Two neoproterozoic crustal accretion events in the Brasília belt, central Brazil," *Journal of South American Earth Sciences*, vol. 18, no. 2, pp. 183–198, 2005.

[99] H. K. Liu, S. S. Gao, P. G. Silver, and Y. Zhang, "Mantle layering across central South America," *Journal of Geophysical Research*, vol. 108, no. 1, p. 2510, 2003.

[100] J. C. Van Decar, D. E. James, and M. Assumpção, "Seismic evidence for a fossil mantle plume beneath South America and implications for plate driving forces," *Nature*, vol. 378, no. 6552, pp. 25–31, 1995.

[101] M. S. M. Mantovani, M. C. L. Quintas, W. Shukowsky, and B. B. de Brito Neves, "Delimitation of the Paranapanema proterozoic block: a geophysical contribution," *Episodes*, vol. 28, no. 1, pp. 18–22, 2005.

[102] R. Unrug, "The Assembly of Gondwanaland," *Episodes*, vol. 19, pp. 11–20, 1996.

[103] U. G. :Cordani, K. Sato, W. Teixeira, C. C. G. Tassinari, and M. A. S. Basei, "Crustal evolution of the South American platform," in *Tectonic Evolution of South America, 31st International Geological Congress, Rio De Janeiro*, U. G. :Cordani, E. J. Milani, A. A. Thomaz Filho, and D. A. Campos, Eds., pp. 19–40, 2000.

[104] U. G. :Cordani, C. C. G. Tassinari, and D. R. Rolim, "The basement of the Rio Apa Craton in Mato Grosso do Sul (Brazil) and northern Paraguay: a geochronological correlation with the tectonic provinces of the south-western Amazonian Craton," in *Gondwana Conference, Abstracts Volume, Mendoza, Argentina*, pp. 1–12, 2005.

[105] A. Kröner and U. Cordani, "African, southern Indian and South American cratons were not part of the Rodinia supercontinent: evidence from field relationships and geochronology," *Tectonophysics*, vol. 375, no. 1–4, pp. 325–352, 2003.

[106] C. B. Prezzi and R. N. Alonso, "New paleomagnetic data from the northern Argentine Puna: central Andes rotation pattern reanalyzed," *Journal of Geophysical Research B*, vol. 107, no. 2, pp. 1–18, 2002.

[107] A. E. Rapalini, "The accretionary history of southern South America from the latest Proterozoic to the Late Palaeozoic: some palaeomagnetic constraints," *Geological Society*, vol. 246, pp. 305–328, 2005.

[108] D. Nürberg and R. D. Müller, "The tectonic evolution of South Atlantic from Late Jurassic to present," *Tectonophysics*, vol. 191, pp. 27–43, 1991.

[109] H. K. Chang, R. O. Kowsmann, and A. M. F. de Figueiredo, "New concepts on the development of east Brazilian marginal basins," *Episodes*, vol. 11, no. 3, pp. 194–202, 1988.

[110] W. S. Holbrook and P. B. Kelemen, "Large igneous province on the US atlantic margin and implications for magmatism during continental breakup," *Nature*, vol. 364, no. 6436, pp. 433–436, 1993.